

Surface/Interface Scattering

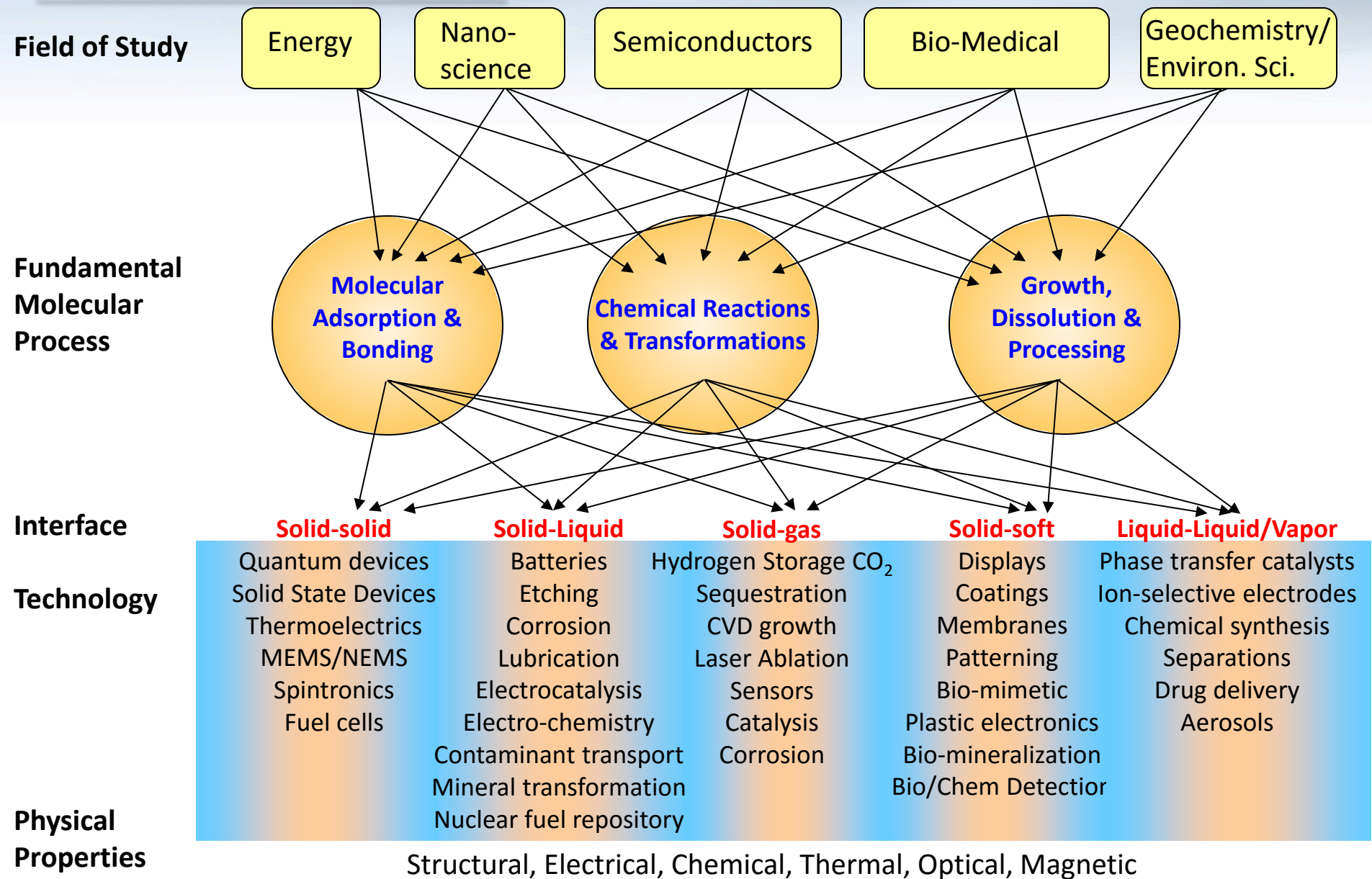
*Paul Zschack, NSLS-II/Brookhaven National Lab
X-ray & Neutron School, 6 August 2017*



Thoughts before we start...

- A 'surface' is actually an interface
- All materials interact with their environment at their surface or interface
- Don't wish to provide depth, nuance, or detailed derivations, but rather a broad tour of applications that provide a view of what's possible today.

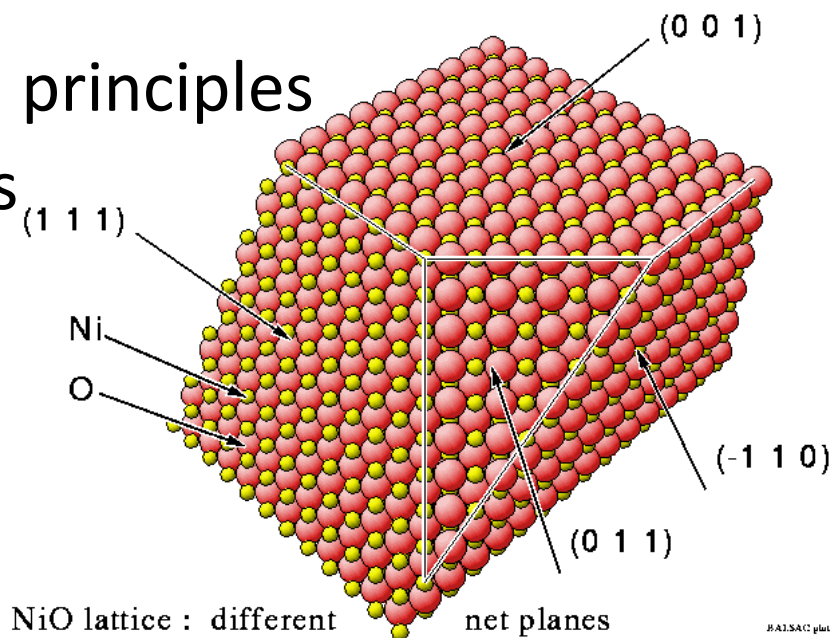
Interfacial Science



Motivations

- Fundamental understanding
- Technology development
 - Electronics
 - Catalysis
 - Separations
- Materials growth & dissolution principles
- New, novel interface properties
- Environmental remediation
- Nano-science

- Why x-rays?



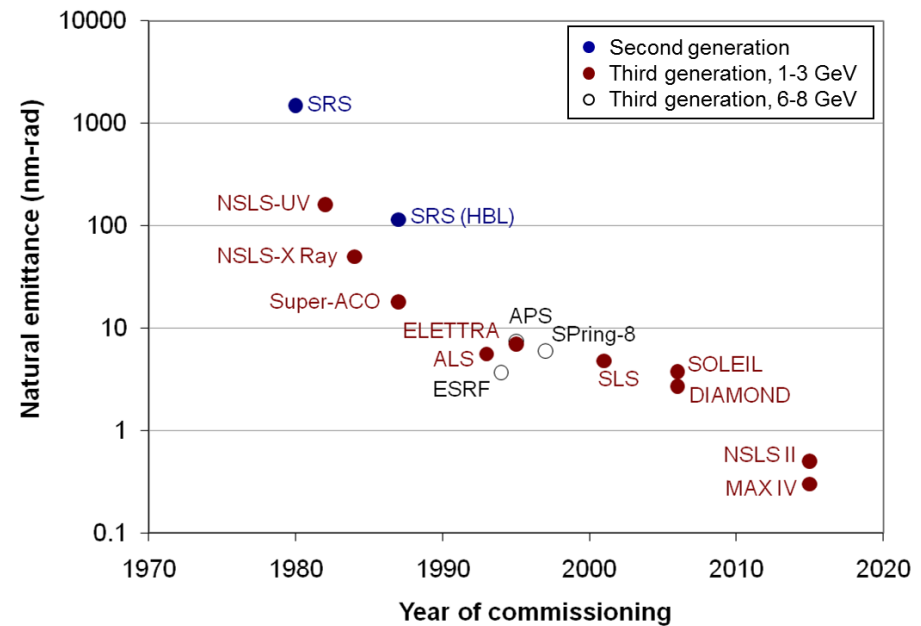
Advantages of using X-Rays

Why x-rays?

- Penetration – In-situ studies possible
- Contrast – elemental sensitivity
- Kinematic – straightforward interpretation

Synchrotrons provide:

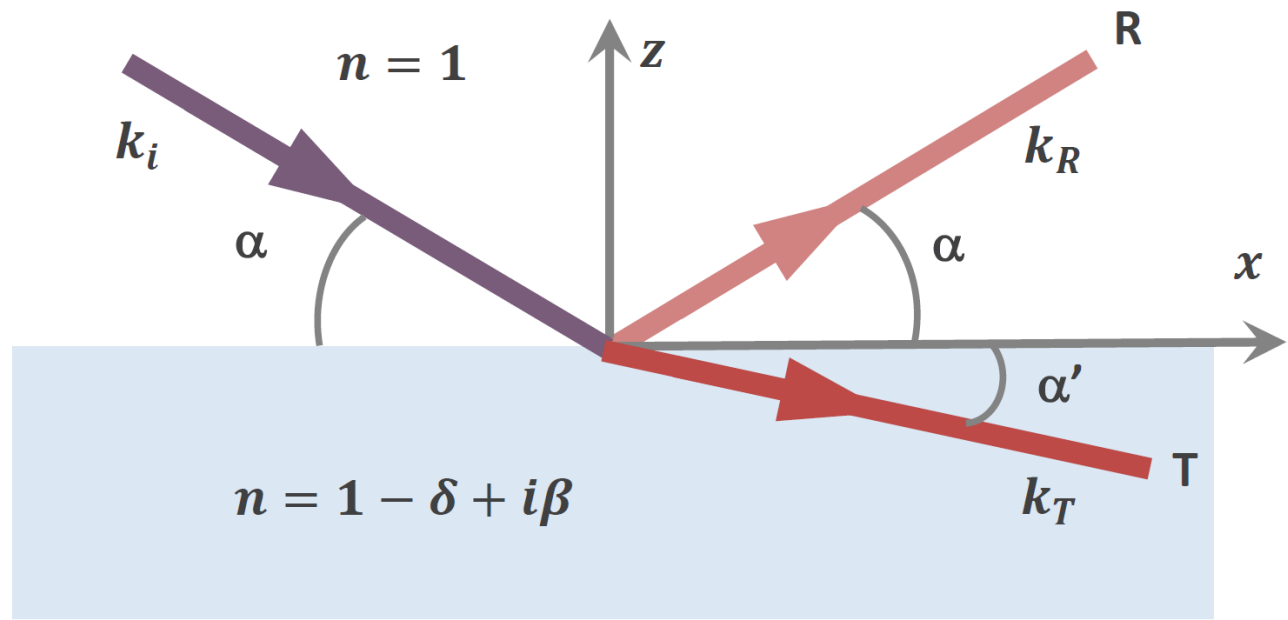
- Flux (and brightness)
- Time-resolution
- Tunability



Outline

- Reflectivity
- Diffraction & in-plane structure
- The crystal truncation rod (CTR)
- Interfacial chemistry
- Materials Synthesis using Pulsed Laser Deposition
- Interface Visualization with X-Ray Reflection Interface Microscopy
 - Application to thin-films
- Surface sensitive coherent x-ray scattering (XPCS, CDI)
- Instruments at light sources for interface science

X-ray reflection and refraction



$$n = 1 - \delta + i\beta$$

$$\delta = \frac{\lambda^2}{2\pi} r_e \rho_e$$

$$\beta = \frac{\lambda}{4\pi} \mu_x$$

Snell's law:

$$\cos \alpha = n \cos \alpha'$$

Critical angle for total external reflection ($\alpha'=0$):

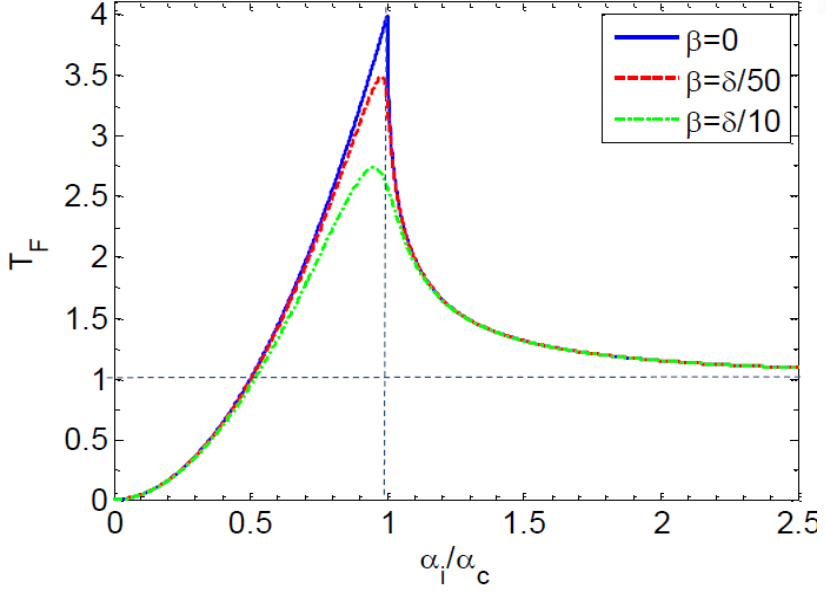
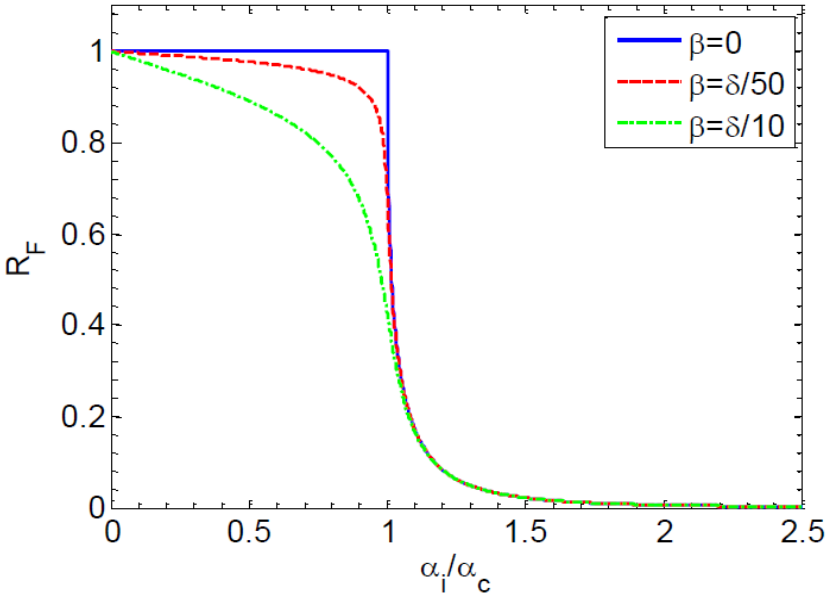
$$\alpha_c = \cos^{-1} n \approx \sqrt{2\delta}$$

Typical $\delta \sim 10^{-5}$, so $\alpha_c \sim 0.1^\circ - 0.5^\circ$

Wave vector transfer for reflected beam

$$q_z = 2k \sin(\alpha)$$

Reflectivity and transmission



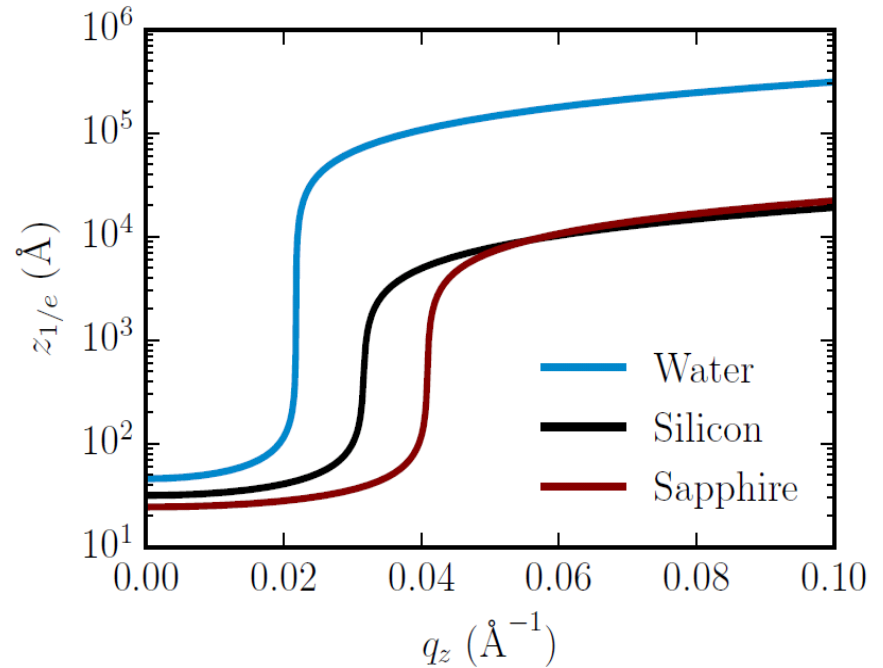
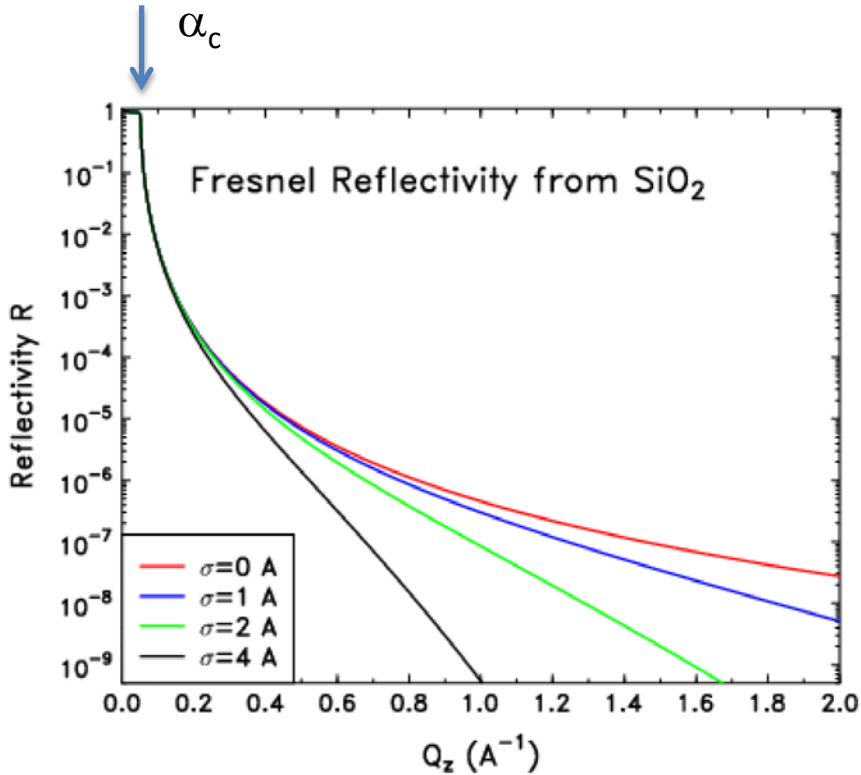
$$T_F = \left| \frac{2\alpha_i}{\alpha_i + \alpha_t} \right|^2 \quad R_F = \left| \frac{\alpha_i - \alpha_t}{\alpha_i + \alpha_t} \right|^2$$

$$n = 1 - \delta + i\beta$$

$$\delta = \frac{\lambda^2}{2\pi} r_e \rho_e$$

$$\beta = \frac{\lambda}{4\pi} \mu_x$$

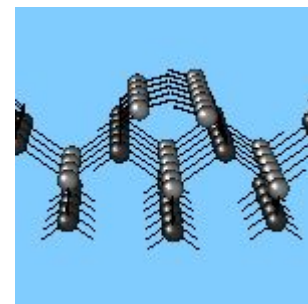
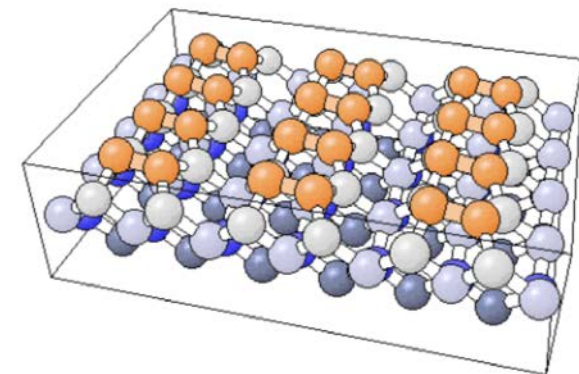
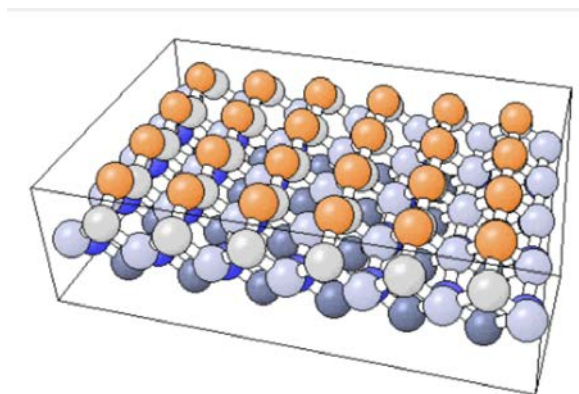
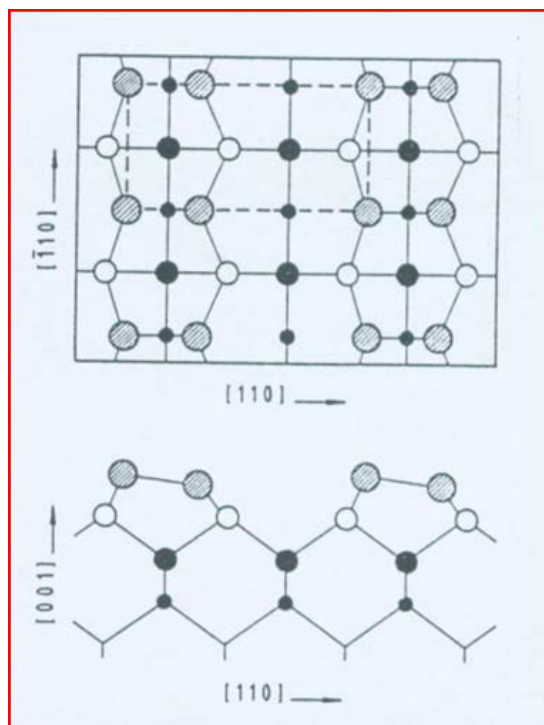
X-ray reflectivity and penetration depth



$$r_{rough} = r_{ideal} e^{-2k_z k'_z \sigma^2}$$

Surface reconstruction – Si (100) 2x1

- Ideally terminated surface may not be lowest energy state – broken symmetry
- Surface reconstructions are widely observed



Grazing incidence surface diffraction

- Grazing incidence provides for reduced bulk scattering and high S/N ratio
- In-plane diffraction can be used to measure surface structure factors and solve the surface structure

H. Dosch, Springer Tracts in Mod. Phys. (Springer), Berlin, 1992, p. 126.

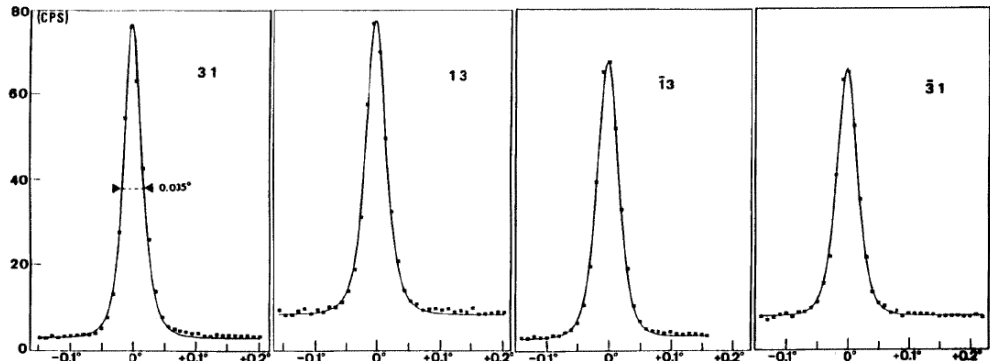
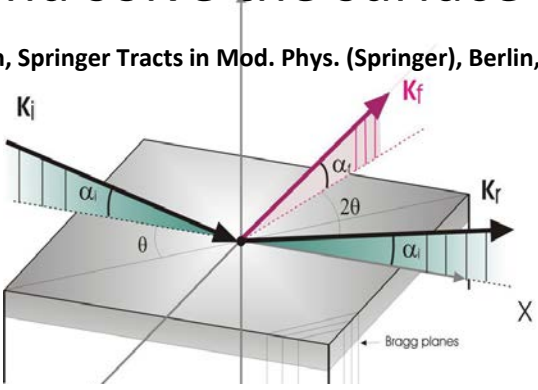


Fig. 3. As/Si(001)2x1 reconstructed surface. Transverse scans of four 31 integer orders with narrow FWHM insensitive to the azimuthal angle. Angular steps: 0.01°

<i>h k</i>	Si(001)2 × 1, 1 × 2		
	<i>F</i> ^{obs}	σ	<i>F</i> ^{calc}
0 3/2	1.56	0.10	1.55
0 5/2	0.53	0.06	0.50
0 3			
1 1/2	0.82	0.08	0.71
1 1			
1 3/2	0.85	0.05	0.87
1 2	1.72	0.06	1.74
1 5/2			
1 3	0.96	0.07	0.96
1 7/2	0.88	0.04	0.88
1 4			
2 1/2	0.65	0.07	0.76
2 3/2	1.24	0.04	1.20
2 5/2	0.40	0.04	0.43
2 3	1.22	0.11	1.28
3 1/2			
3 3/2			

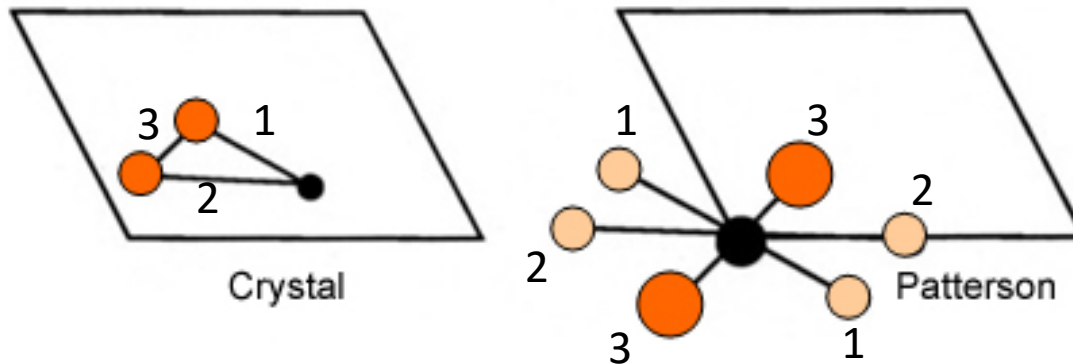
$\chi^2 = 1.30$
 $B_{Si} = 1.0 (\pm 0.1)$

Patterson synthesis

- Patterson Function corresponds to a map of position vectors (relative positions) between each pair of atoms in the structure.
- The Patterson function is equivalent to the electron density convoluted with its inverse.

$$P(\vec{u}) = \rho(\vec{r}) * \rho(-\vec{r}).$$

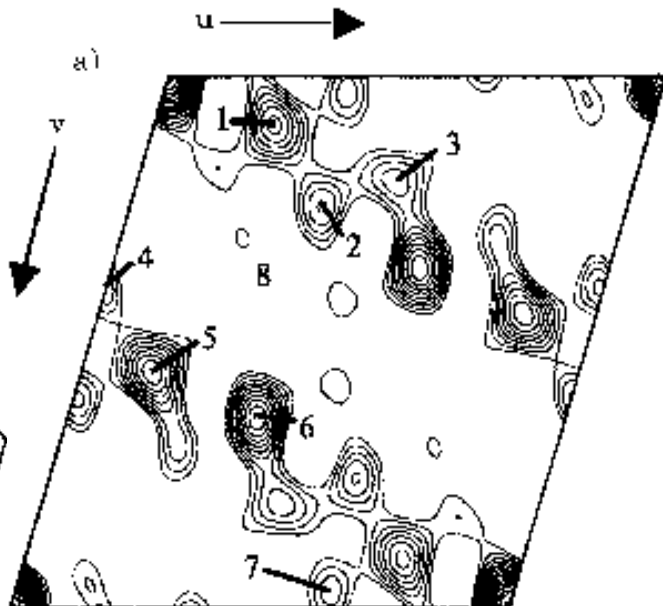
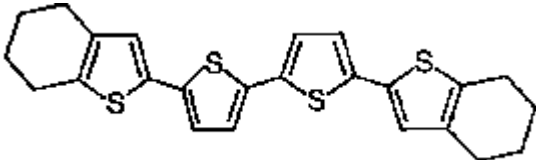
$$P(xy) = \frac{1}{a} \sum_{hk} |F_{hk}|^2 \cos[2\pi(hx + ky)]$$



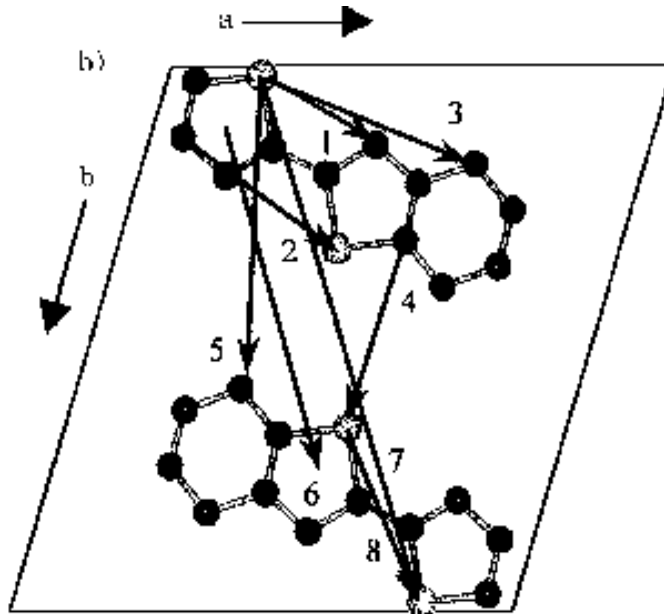
Patterson synthesis (2)

- Large π -conjugated organic molecule adsorbed on a metallic surface (end-capped quaterthiophene on Ag(111))
- Previous belief was that organic molecules absorbed on weakly interacting surfaces remain essentially undistorted
- Result of this study showed significant distortion of the thiophene rings and elongation of the bond distances.

Patterson-function $P(u,v)$ for EC4T/Ag(111).



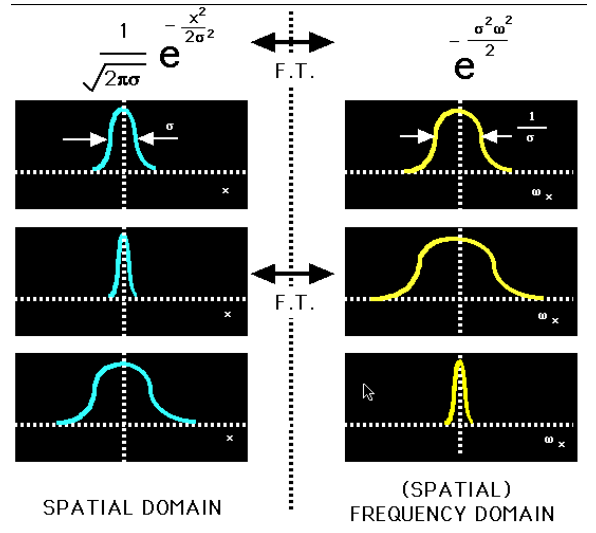
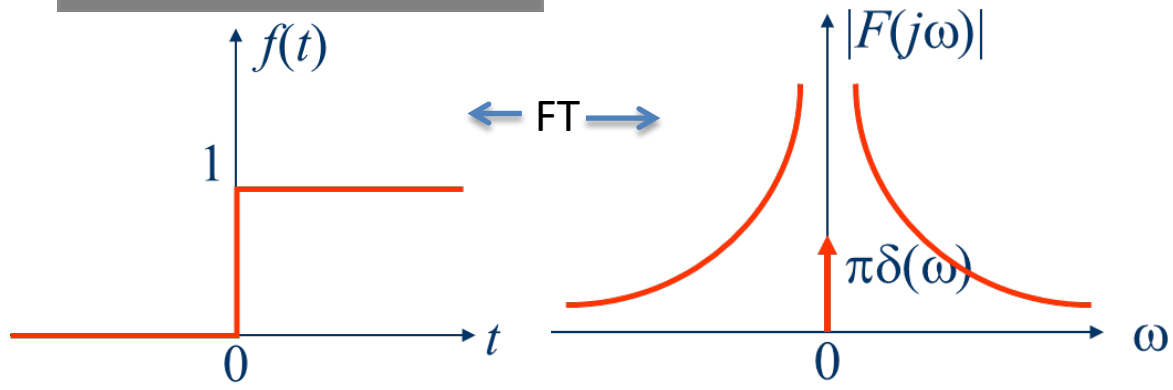
H. L. Meyerheim *et al* 2000 *Europhys. Lett.* 52 144



Reciprocal space

- Large things in real space are sharp (small) in reciprocal space. So, a large single crystal gives rise to very sharp Bragg peaks.
- Small things in real space are broad in reciprocal space. Very small crystals have broad diffraction peaks.
- A plane in real space is a line in reciprocal space. So the scattering from a 2D plane in real space is a 1-dimensional line in reciprocal space.

$$u(t) \xleftrightarrow{F} \pi\delta(\omega) + \frac{1}{j\omega}$$



Review of scattering equations

$$E(\mathbf{R}) \propto FT[\rho(\mathbf{r})] = \sum_{\mathbf{n}} f_{\mathbf{a},\mathbf{n}} e^{i\mathbf{Q}\cdot\mathbf{r}_{\mathbf{n}}}$$

$$E \propto \sum_{n_1=-\frac{(N_1-1)}{2}}^{\frac{(N_1-1)}{2}} e^{i2\pi n_1 H} \sum_{n_2=-\frac{(N_2-1)}{2}}^{\frac{(N_2-1)}{2}} e^{i2\pi n_2 K} \sum_{n_3=-\frac{(N_3-1)}{2}}^{\frac{(N_3-1)}{2}} e^{i2\pi n_3 L} \sum_{j=1}^m f_{\mathbf{a},j} e^{i\mathbf{Q}\cdot\mathbf{r}_j} e^{-M_j}$$

Sum over n_1
 N_1 total cells
 ↓
 $(N_1-1)/2$
 $-(N_1-1)/2$

Sum over n_2
 N_2 total cells
 ↓
 $(N_2-1)/2$
 $-(N_2-1)/2$

Sum over n_3
 N_3 total cells
 ↓
 $(N_3-1)/2$
 $-(N_3-1)/2$

Sum over the m
 atoms in the unit cell
 ↓
 $j=1$
 m

Thermal disorder parameter
 ↖
 e^{-M_j}

Structure factor of the unit cell

$$F_c = \sum_{j=1}^m f_{\mathbf{a},j} e^{i\mathbf{Q}\cdot\mathbf{r}_j} e^{-M_j}$$

Slit Function

$$S_1 = \sum_{n_1=-\frac{(N_1-1)}{2}}^{\frac{(N_1-1)}{2}} e^{i2\pi n_1 H} = \frac{\sin(N_1\pi H)}{\sin(\pi H)}$$

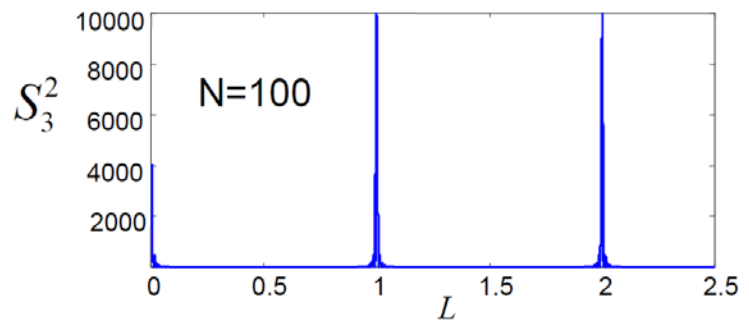
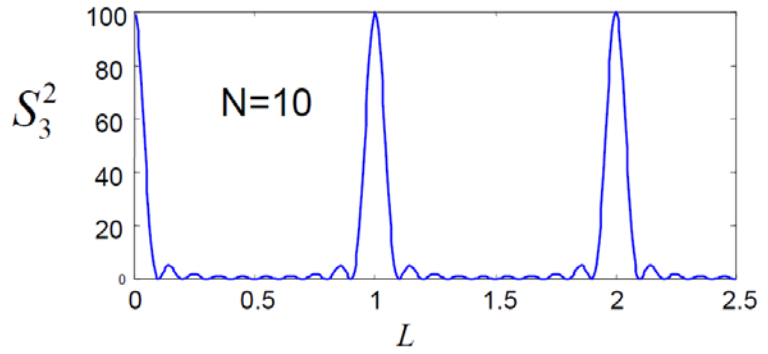
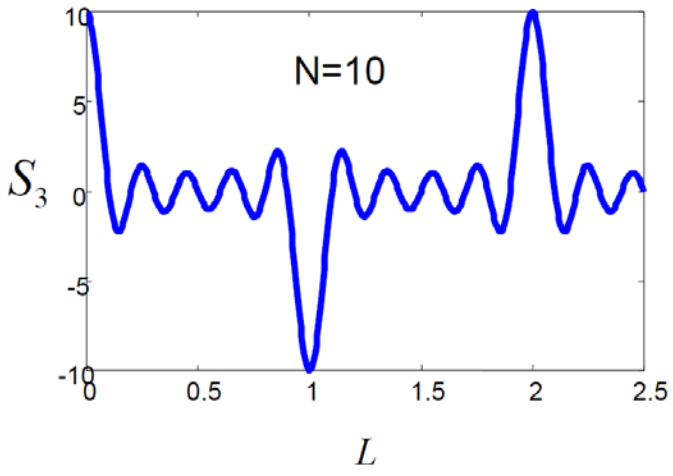
→ N_1 as $H \rightarrow$ integer

$$I \propto |E|^2 \propto |F_c|^2 \frac{\sin^2(N_1\pi H)}{\sin^2(\pi H)} \frac{\sin^2(N_2\pi K)}{\sin^2(\pi K)} \frac{\sin^2(N_3\pi L)}{\sin^2(\pi L)} \rightarrow |F_c|^2 N_1^2 N_2^2 N_3^2$$

For $(HKL) \rightarrow$ integer

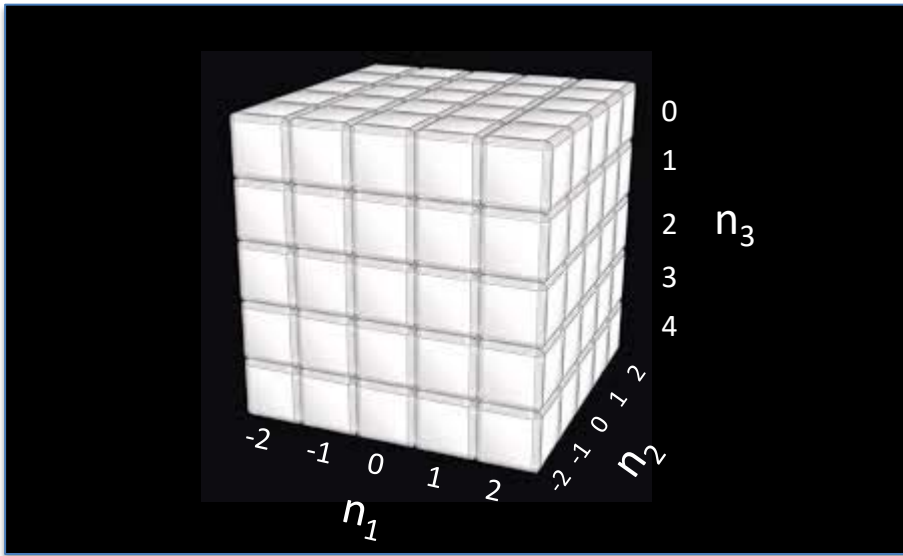
Slit interference function

$$S_3(L) = \sum_{-(N_3-1)/2}^{(N_3-1)/2} e^{i2\pi n_3 L} = \frac{\sin(N_3\pi L)}{\sin(\pi L)} \rightarrow N_3 \text{ as } L \rightarrow \text{integer}$$



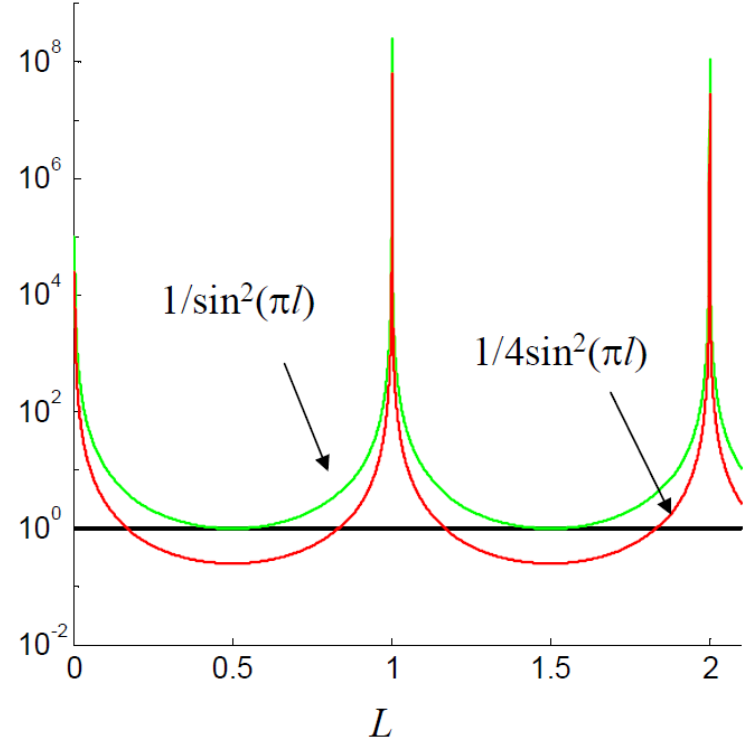
Intensity is nominal for non-integer values. But its not zero if the xtal is finite size!

Lattice factor for terminated surface



$$E \propto F_c \sum_{-(N_1-1)/2}^{(N_1-1)/2} e^{i2\pi n_1 H} \sum_{-(N_2-1)/2}^{(N_2-1)/2} e^{i2\pi n_2 K} \sum_{-\infty}^0 e^{i2\pi n_3 L}$$

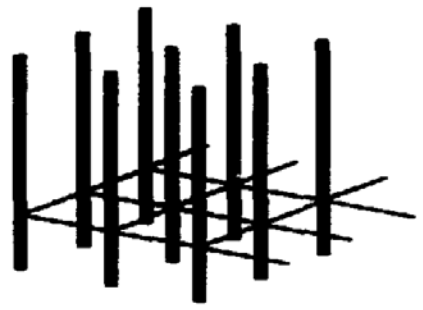
$$F_{ctr} = \sum_{-\infty}^0 e^{i2\pi n_3 L} = \frac{1}{(1 - e^{-i2\pi L})}$$



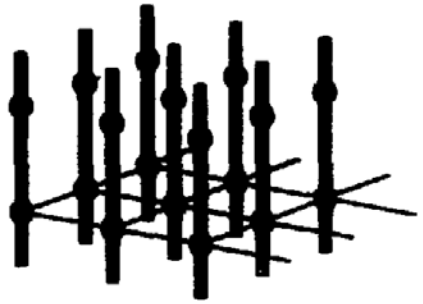
$$I \propto N_1^2 N_2^2 |F_c(HKL)|^2 |F_{CTR}(L)|^2$$

$$|F_{ctr}|^2 = \frac{1}{4 \sin^2(\pi L)}$$

The crystal truncation rod (CTR) intensity



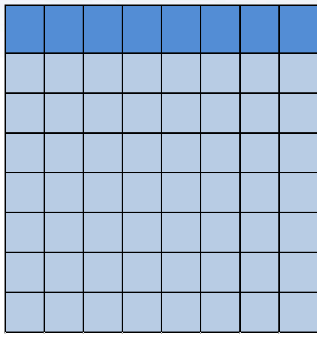
2D LAYER ONLY



BULK CRYSTAL AND 2D LAYER



CRYSTAL TRUNCATION RODS



Surface Unit Cells

Bulk Unit Cells

$$E_T = E_{\text{bulk}} + E_{\text{surf}}$$

$$E_{\text{bulk}} = N_1 N_2 F_{c, \text{bulk}}(HKL) F_{\text{CTR}}(L)$$

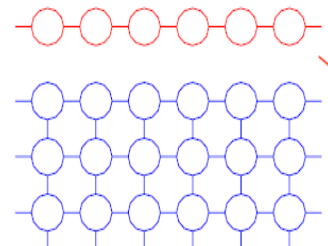
$$E_{\text{surf}} = N_1 N_2 F_{c, \text{surf}}(HKL) e^{i2\pi L}$$

$$I \propto N_1^2 N_2^2 \left| F_{\text{bulk},c} F_{\text{CTR}}(L) + F_{\text{surf},c} \right|^2$$

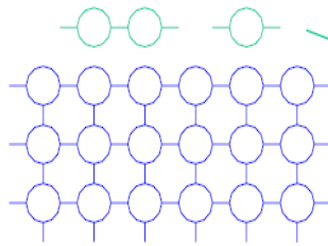
$$F_c = \sum_{j=1}^n f_j e^{i\mathbf{Q}\cdot\mathbf{r}_j} e^{-M_j} \quad \mathbf{Q}\cdot\mathbf{r}_j(xyz) = 2\pi(xH + yK + zL)$$

CTR intensity profile provides exquisite sensitivity

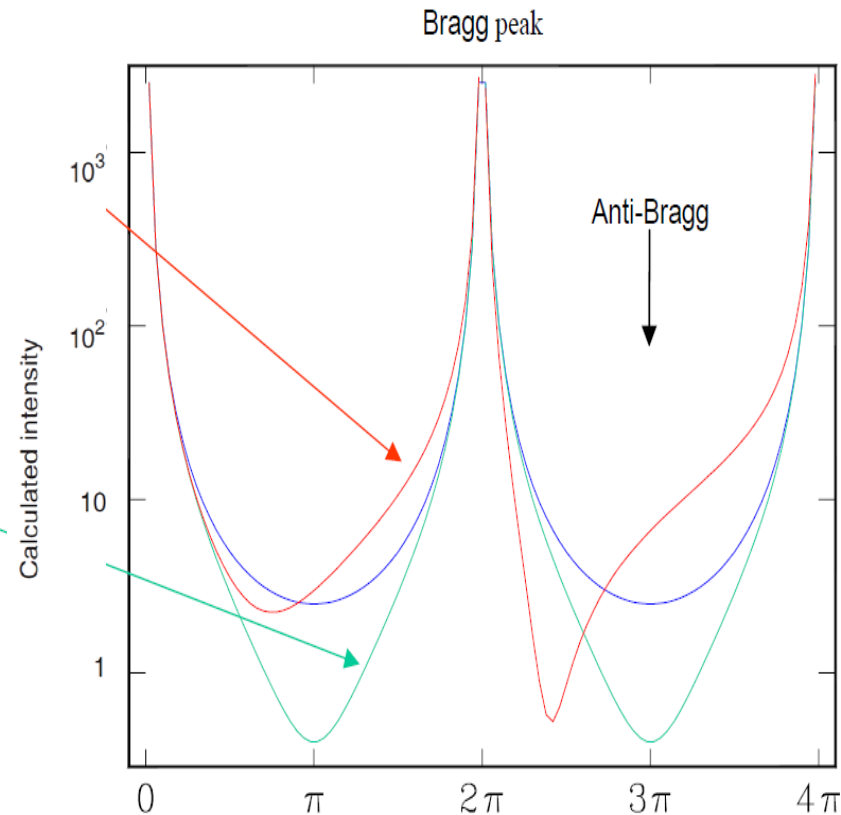
- Observe several orders of magnitude intensity variation with changes in surface:
 - atomic site occupancy
 - relaxation (position)
 - presence of adatoms
 - roughness



EXPANDED LAYER

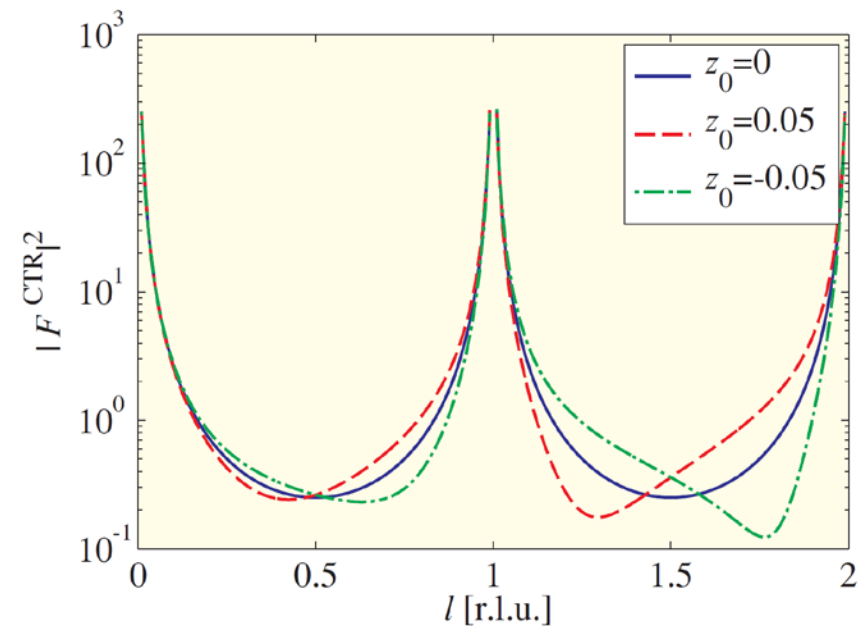
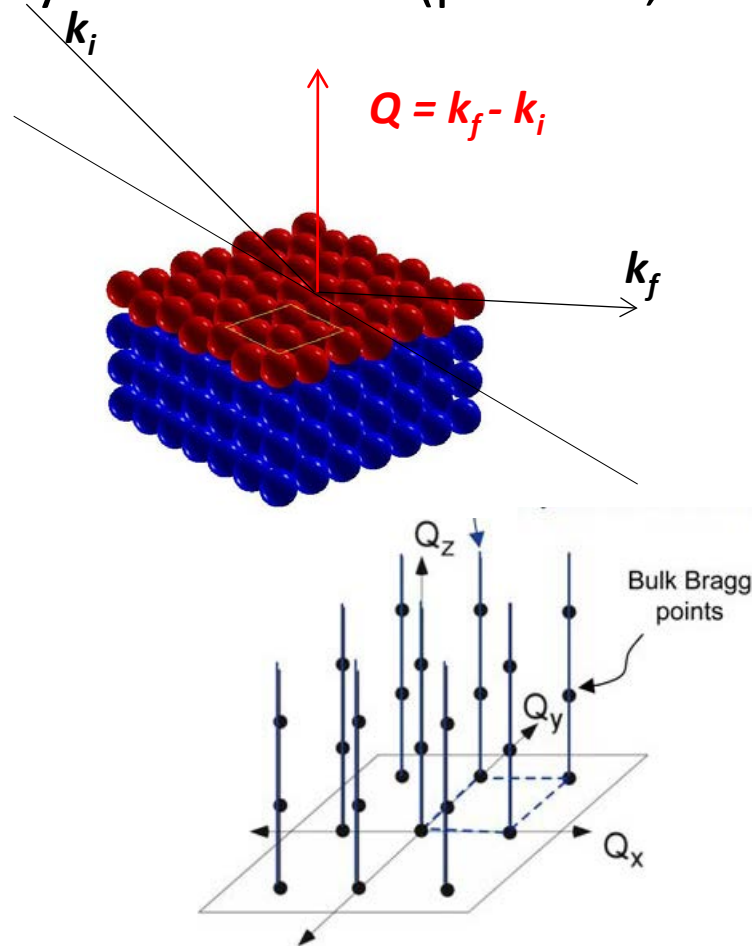


ROUGH SURFACE



X-Ray Techniques – Crystal Truncation Rods (CTR)

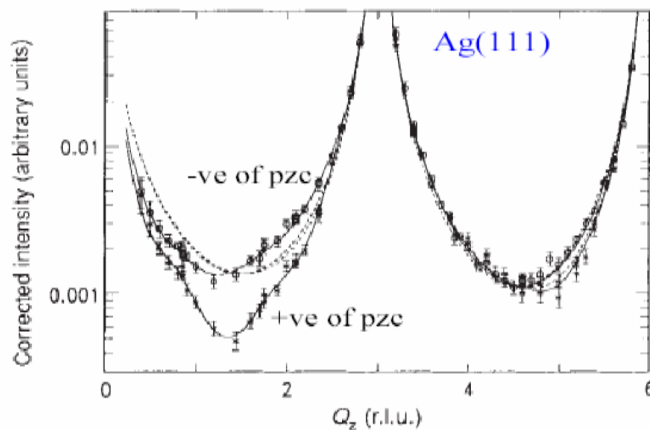
- Crystal Truncation Rod intensity profile is incredibly sensitive to top layer conditions (position, composition, width, etc...)



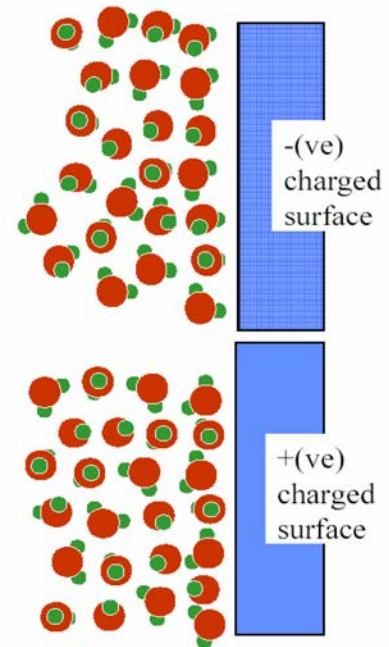
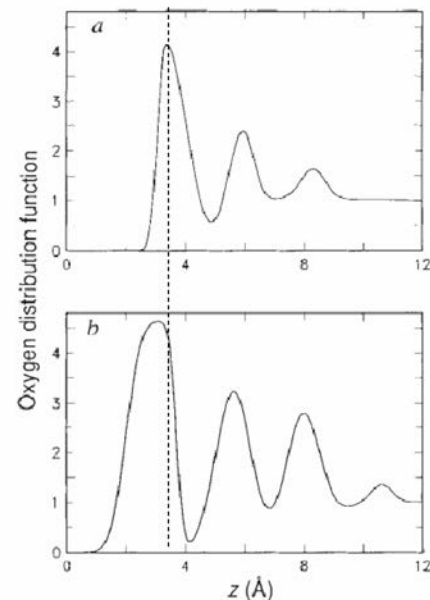
Elements of Modern X-ray Physics
Jens Als-Nielsen, Des McMorrow,
Fig 4.17

CTR analysis applied to water – electrode interface

- Findings show water molecules ordered for about 3 molecular diameters from the electrode
- Spacing for the first layer shows oxygen up (down) average orientation for negative (positive) charge.
- First layer has greater density than bulk water implying the disruption of hydrogen bonding at the interface



Toney et al., Nature **368**, 444 (1994)

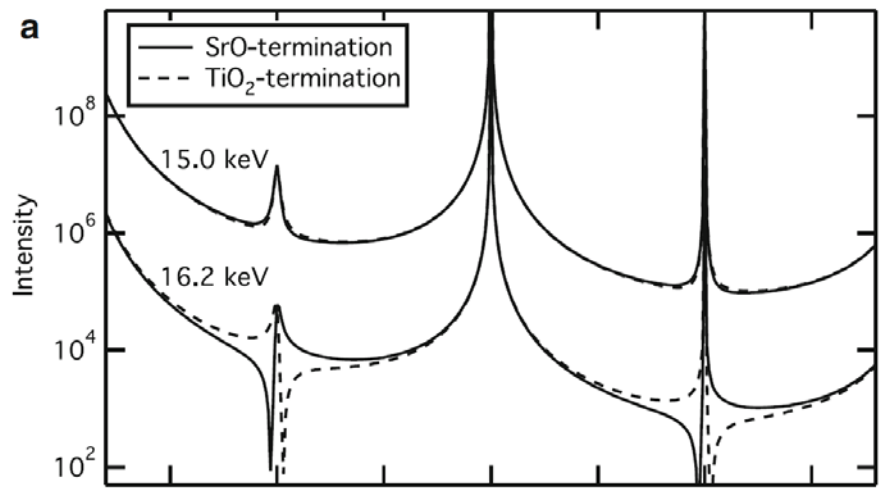
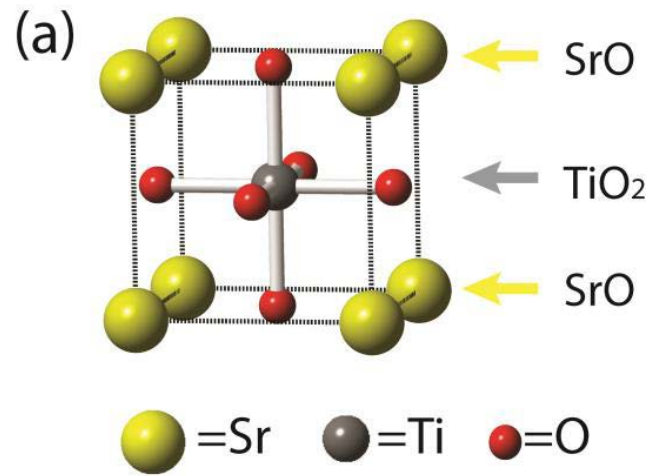
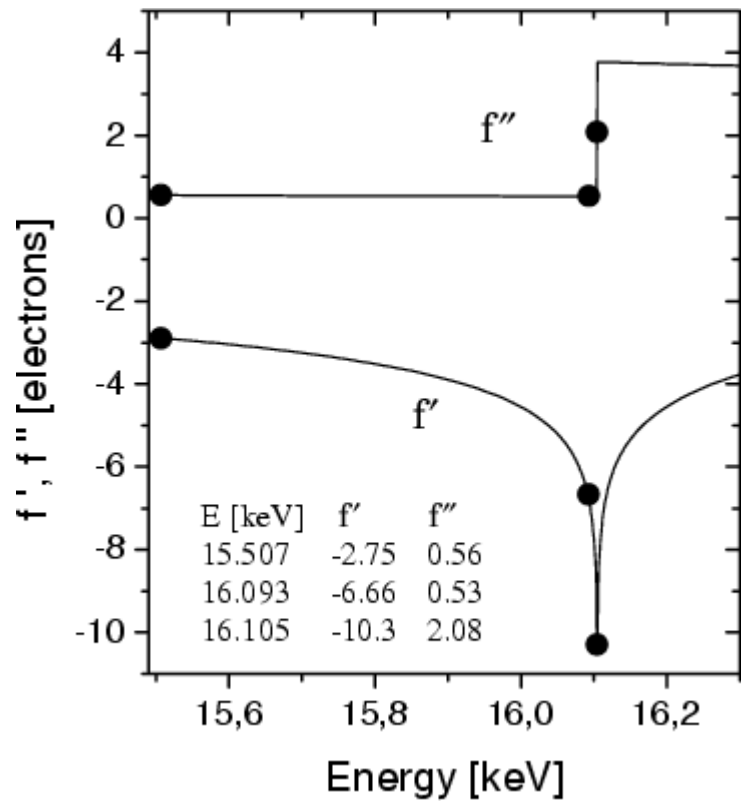


Anomalous scattering contrast

Structure factor of the unit cell

$$F_c = \sum_{j=1}^m f_{a,j} e^{i\mathbf{Q}\cdot\mathbf{r}_j} e^{-M_j}$$

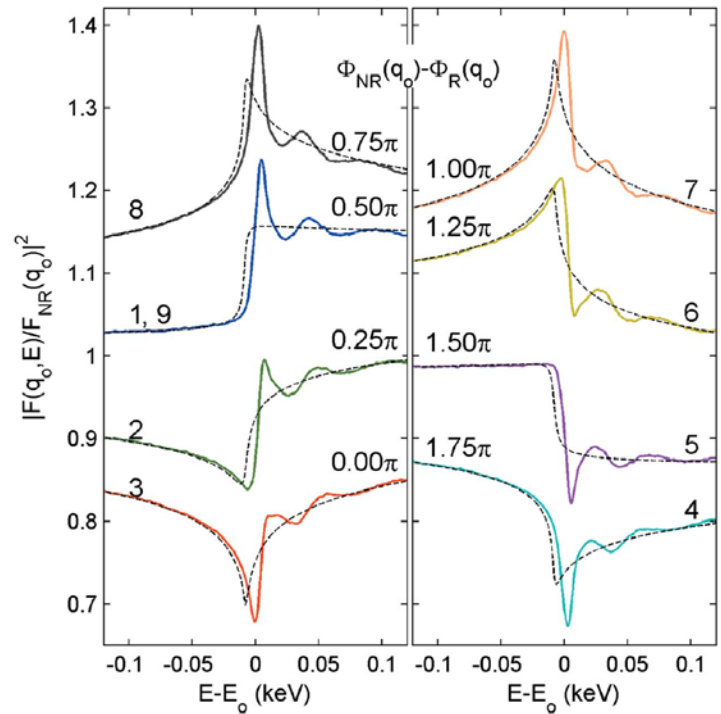
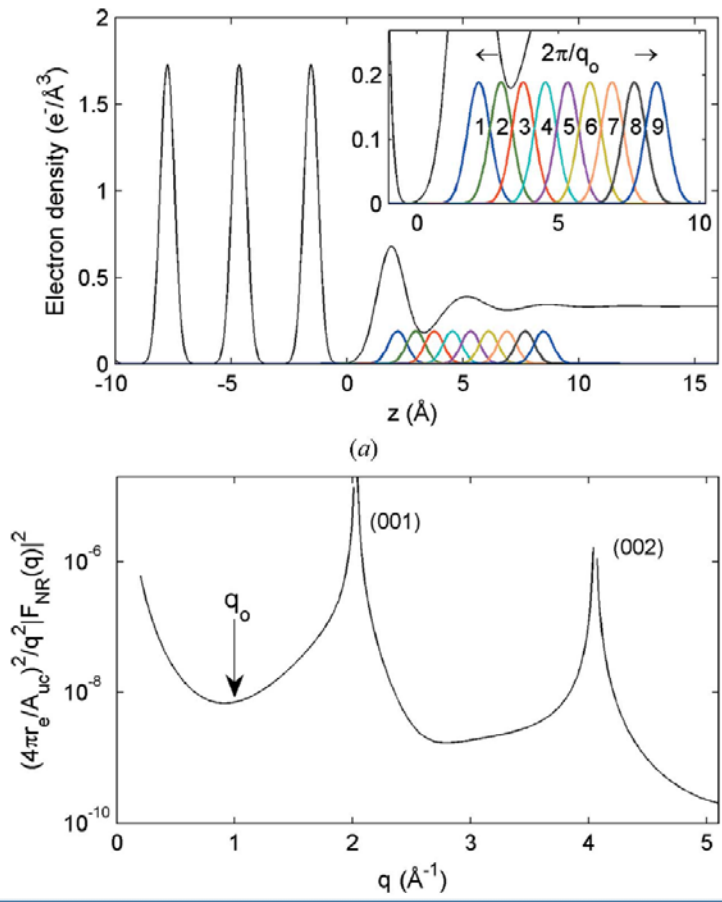
$$f(q,E) = f_0(q) + f'(E) + if''(E)$$



Tim T. Fister and Dillon D. Fong. Thin Film Metal-Oxides: Fundamentals and Applications in Electronics and Energy, Shriram Ramanathan Ed.

Anomalous scattering energy scans at fixed q

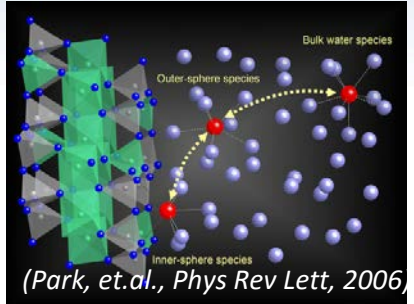
- Simulation of Sr in solution near a quartz interface
- Method used to determine model-independent structures



Park & Fenter, *J. Appl. Cryst.* (2007). **40**, 290–301

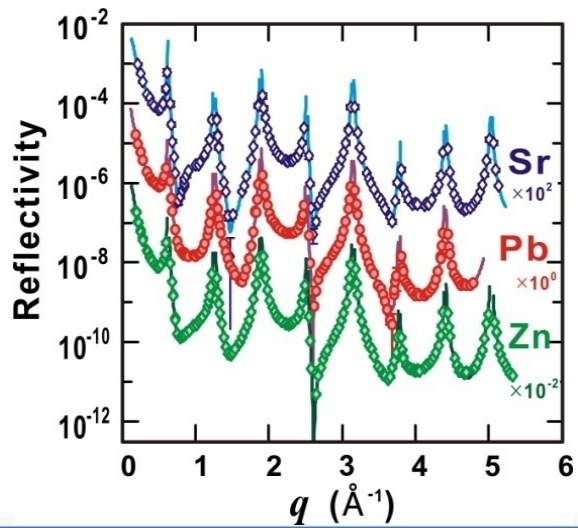
Interfacial chemistry – cation adsorption

- Scattering near an absorption edge provides elemental sensitivity
- Model-independent elemental distributions determined from the resonant reflectivity data
- Adsorption involves distinct species controlled by the cation hydration enthalpy

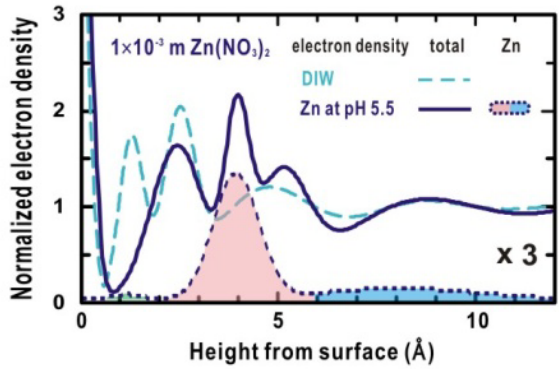
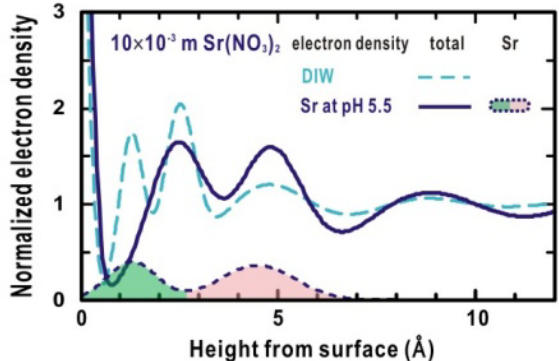
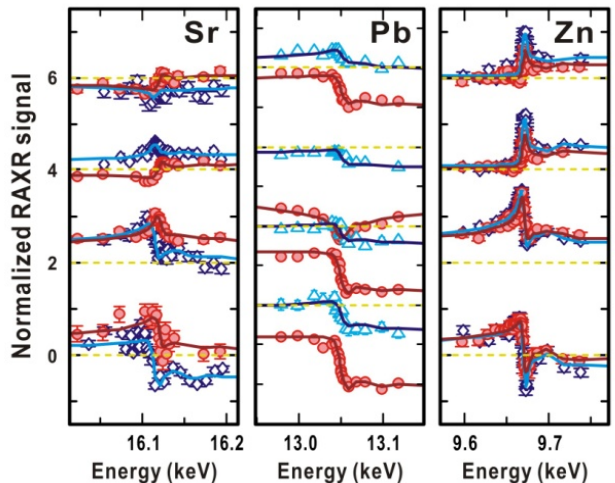


Cation adsorption at the muscovite-electrolyte interface

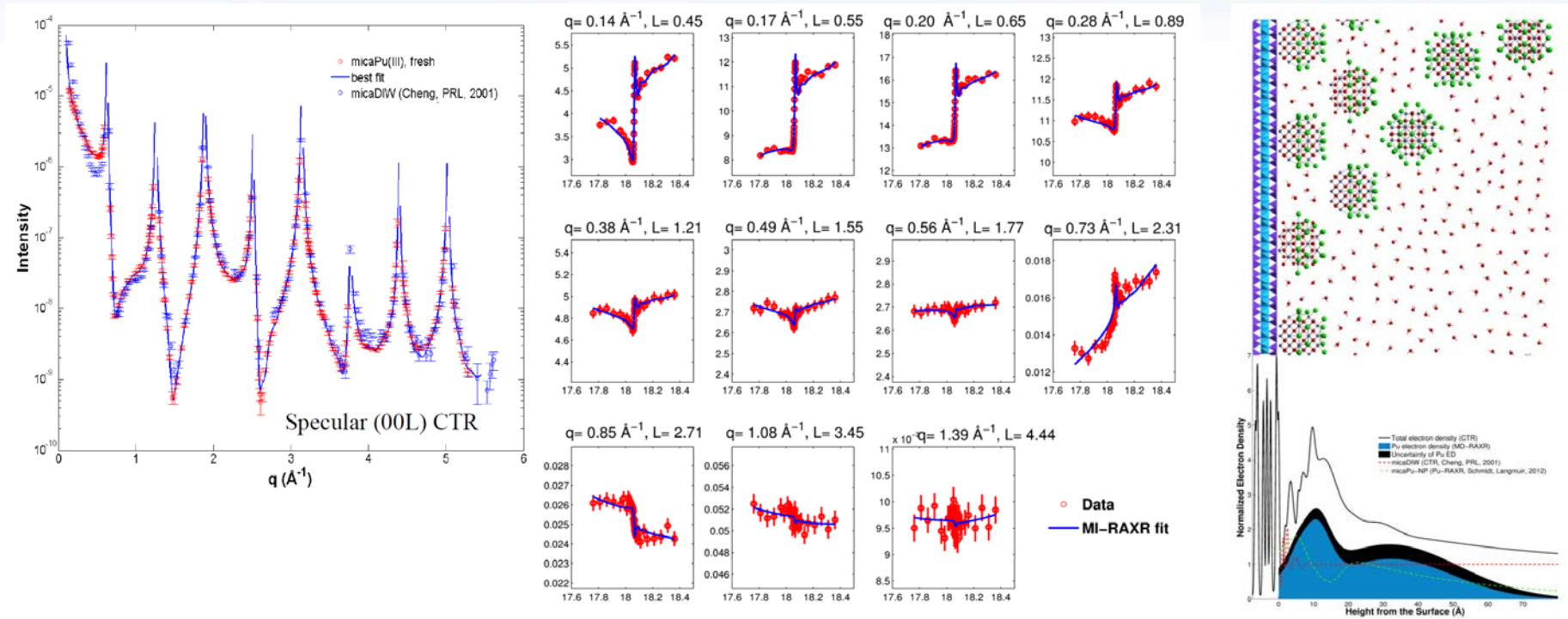
$R(q)$ reveals the **total** interfacial density profile



$R(E)$ reveals the **element-specific** density profile



Surface-mediated formation of Pu nanoparticles

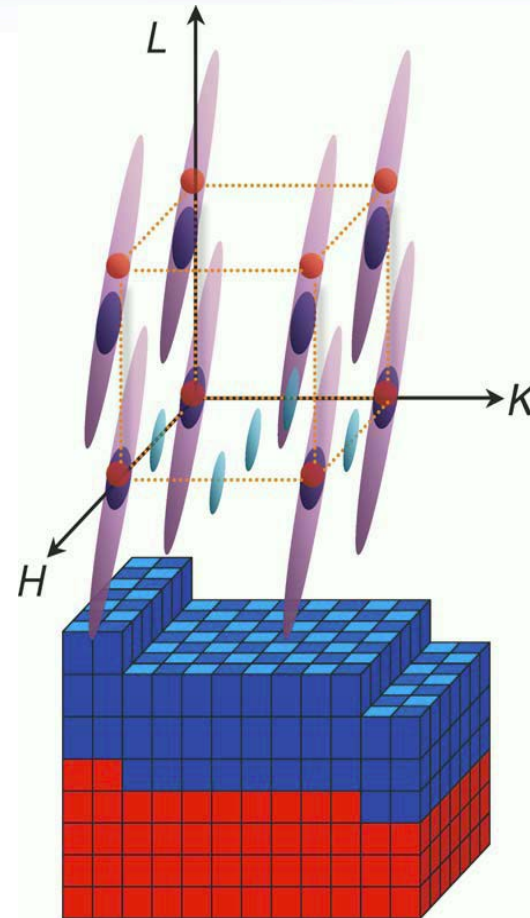


- Pu has broad vertical distribution, peaked at 10.5 Å and extends >70 Å
- Total plutonium coverage >9 Pu/muscovite unit cell (0.77 μg Pu/cm²)
- This type of information can inform remediation strategies

M. Schmidt, et al. *ES&T* 47(24) 14178-14184 (2013)

Scattering/diffraction from high quality films

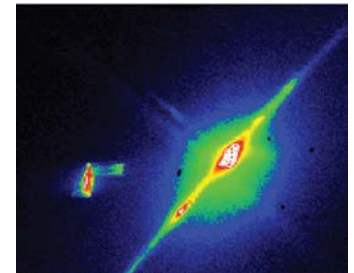
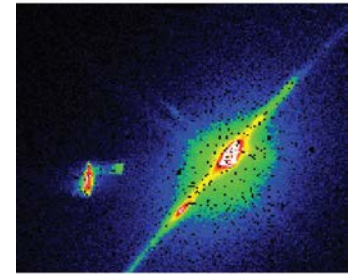
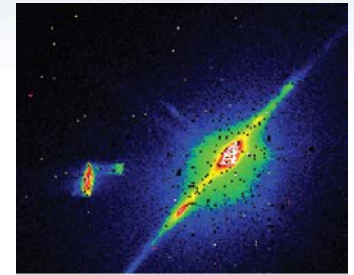
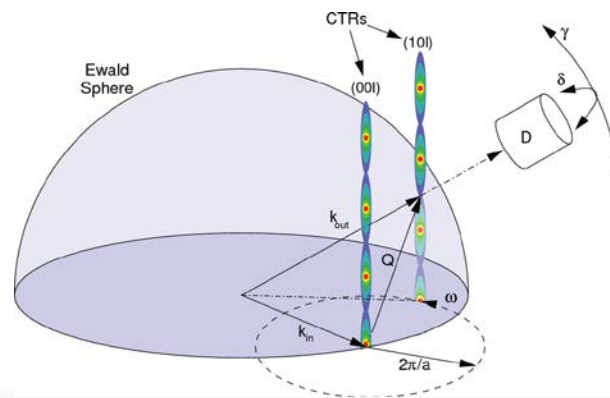
- Diffraction scattering from thin films can be rather complex
- Strained films diffract to different reciprocal space locations
- Thin film diffraction peaks are broadened along 'z'
- Reconstructions produce superlattices with different periodicity
- Surfaces that are miscut from the lattice produce tilted crystal truncation rods



Fong and Thompson, *Annu. Rev. Mater. Res.* (2006)

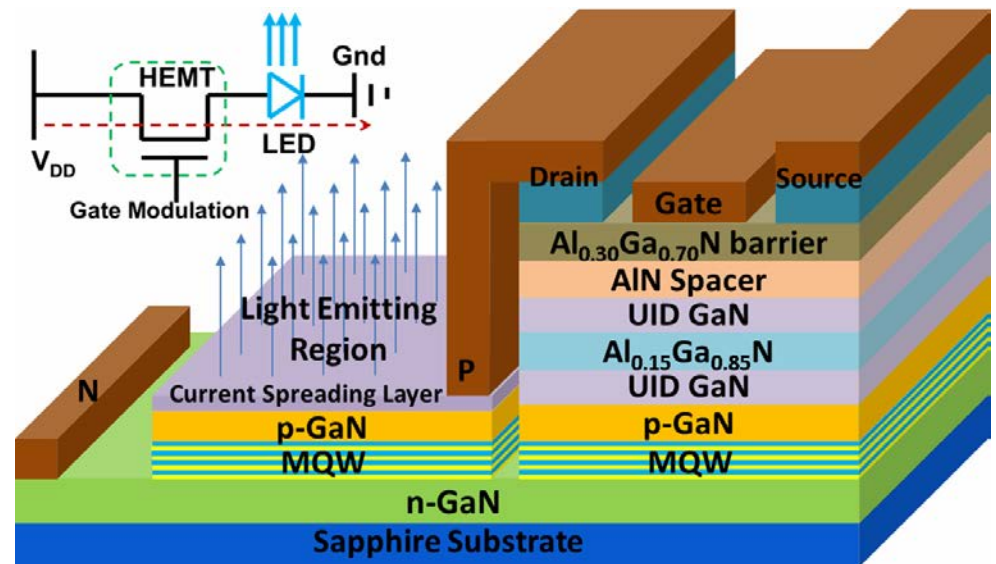
CTR data collection

- Area detectors allow efficient collection of CTR data
- Generally, CTRs are rotated through the Ewald sphere to probe different parts of the rod
- Specular rods provide access to information concerning conditions normal to the surface only
- Non-specular CTRs provide information about lateral registry too



Materials growth

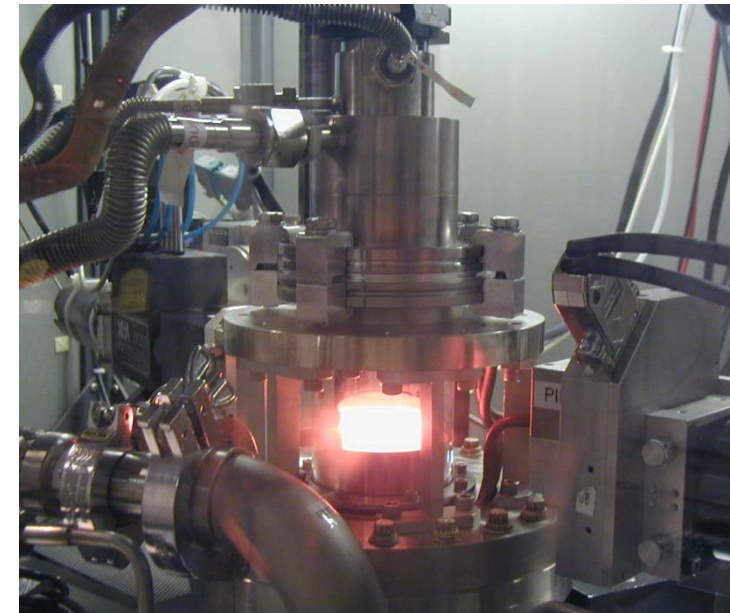
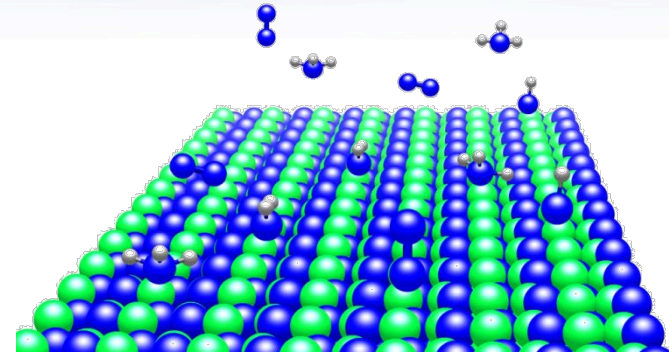
- Vapor phase epitaxy
- Liquid phase epitaxy
- Molecular beam epitaxy
- Sputtering
- Evaporation
- Pulsed laser deposition
- Atomic layer deposition
- Chemical vapor deposition



<http://www.ece.ust.hk/~ptc/research.php>

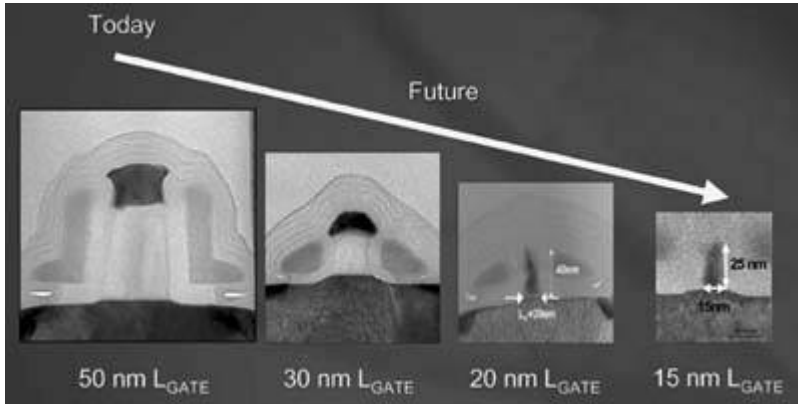
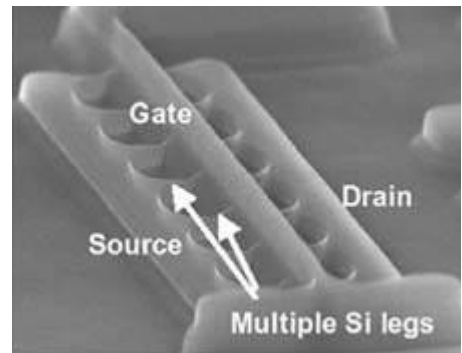
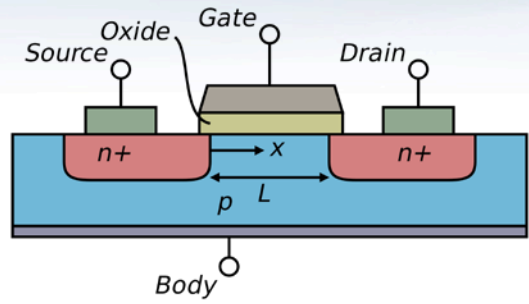
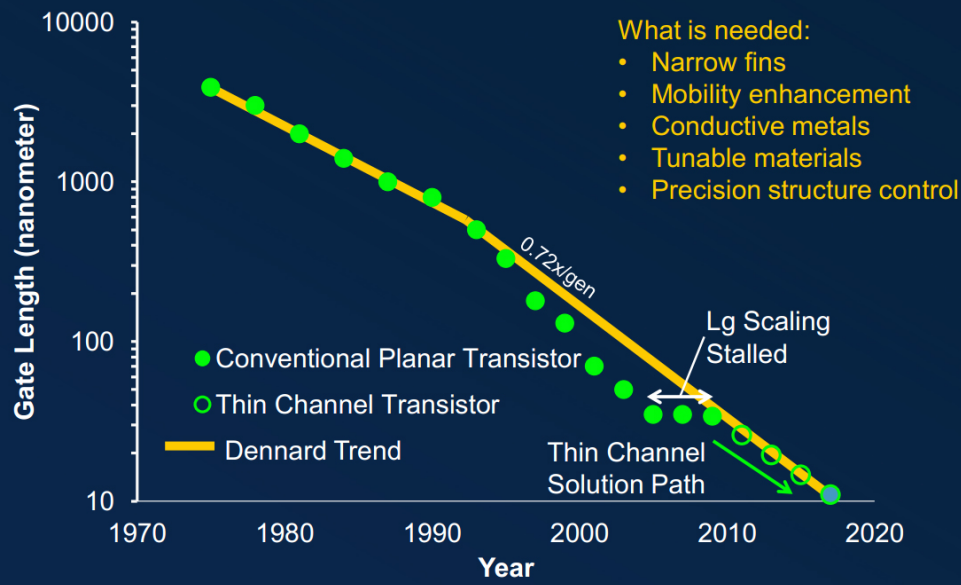
Challenges in materials growth and processing

- Discovery of new materials with new properties and functionality, e.g.
 - Highly efficient lighting
 - New catalysts
 - High performance batteries and fuel cells
- Exciting areas of current interest:
 - complex oxides with emergent properties
 - quantum confined structures
 - Nano-structures
- *In situ* x-ray techniques are powerful tools
 - structure-property relations
 - operating or native conditions
 - materials synthesis
 - etching & dissolution



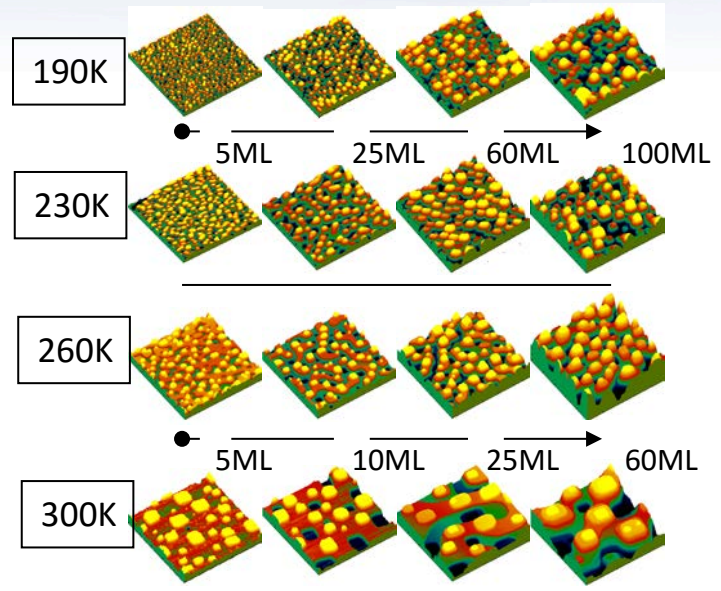
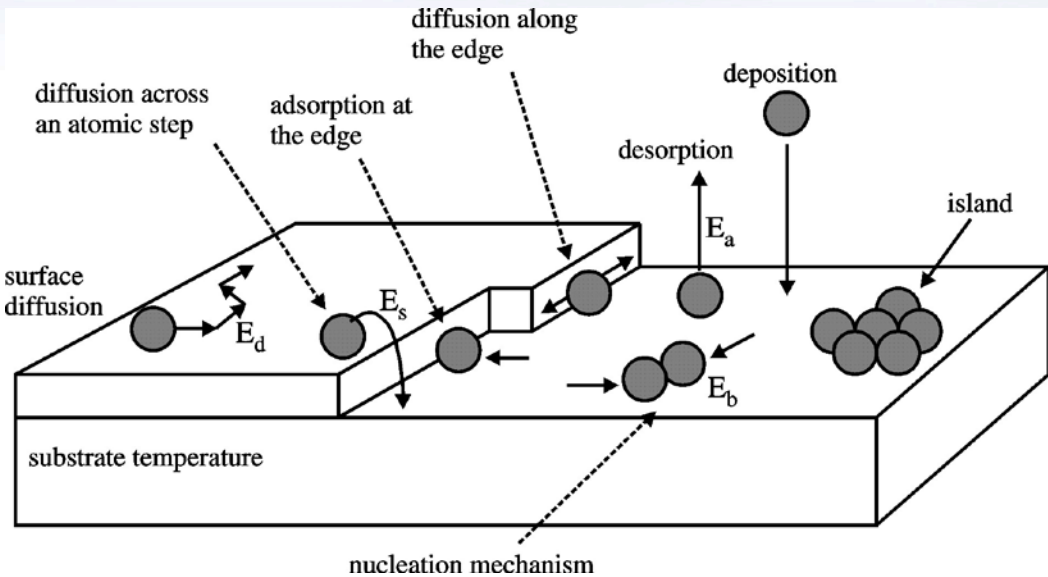
Transistor gate length reduction

Continue The Lg Scaling Path

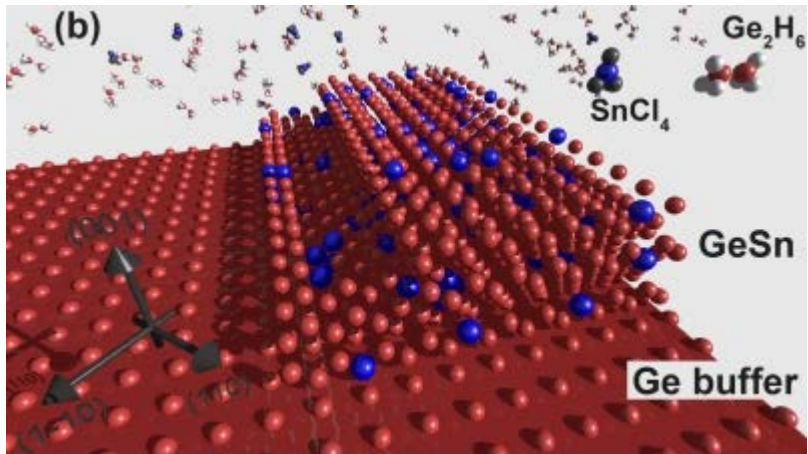


Semiconductor Foundry Market: \$48.8B in 2015

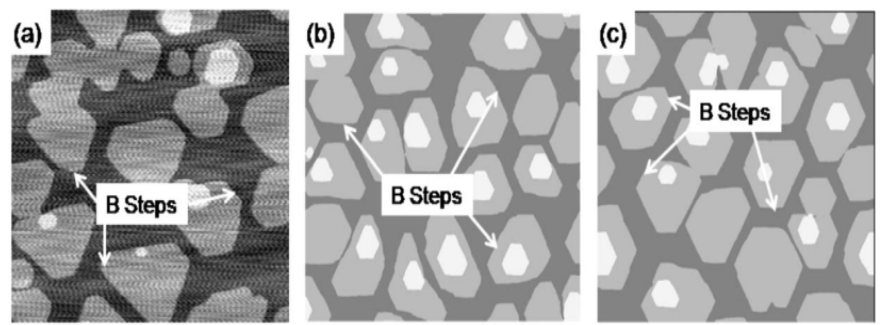
Understanding growth processes & morphology



Jim Evans, Iowa State Univ (2005)



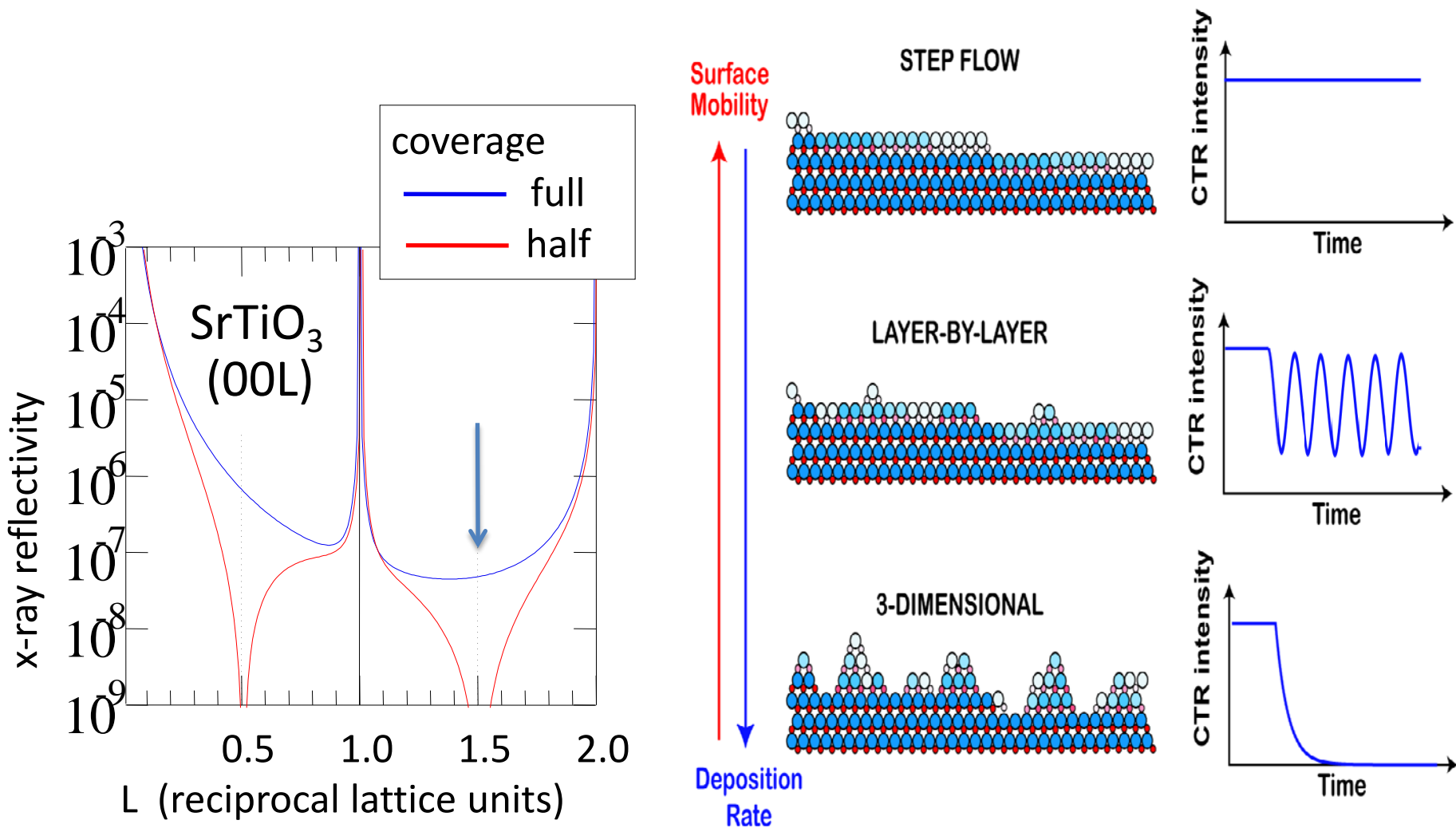
Modeling for Ag on Ag(111)



Maozhi Li, et. Al., Phys. Rev. B, 77, 033402 (2008)

X-Ray techniques – determination of growth modes

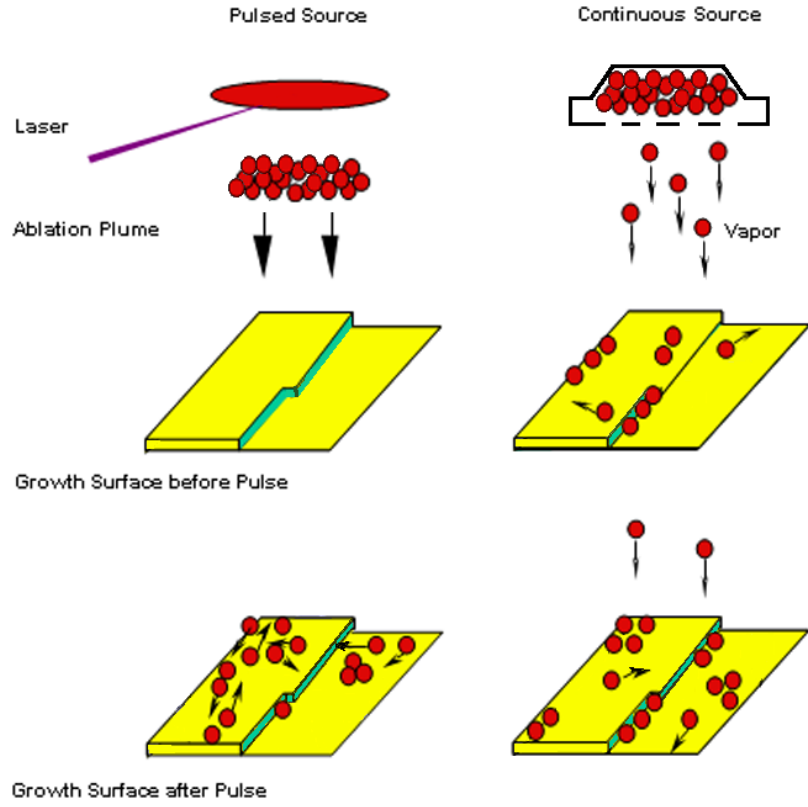
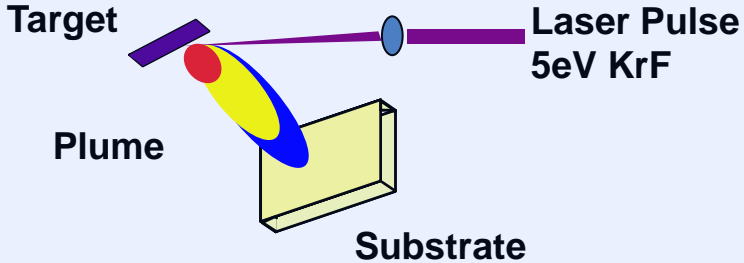
- We can determine growth mode by observation of CTR intensity during growth



Pulsed-Laser Deposition (PLD)

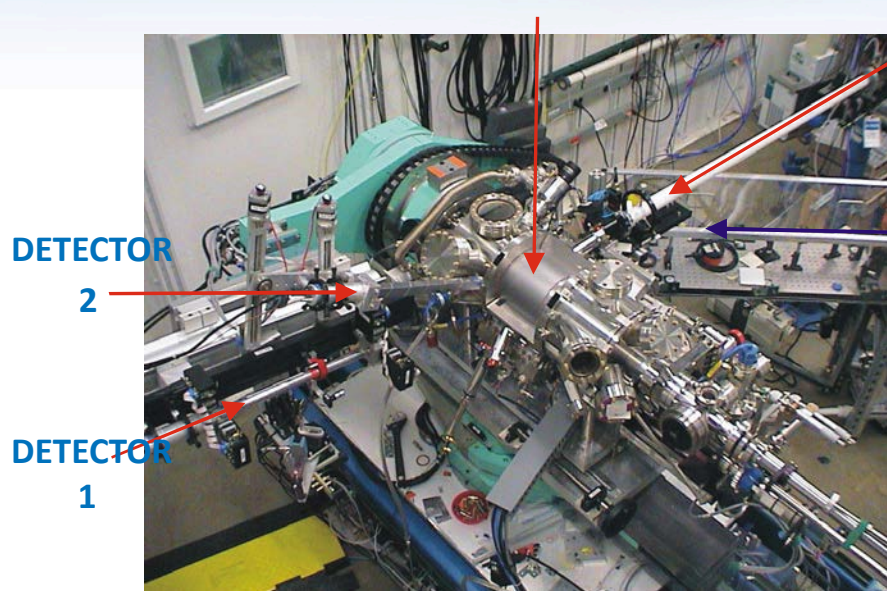
- The PLD process has a number of characteristics that are fundamentally advantageous for the study of the kinetics of crystal growth far from equilibrium:
- In PLD, the affects of material deposition can be separated in time from surface evolution

PLD consists of periodic bursts of highly driven growth followed by relatively long periods of uninterrupted surface relaxation, permitting these two competing processes to be isolated from each other and studied separately.



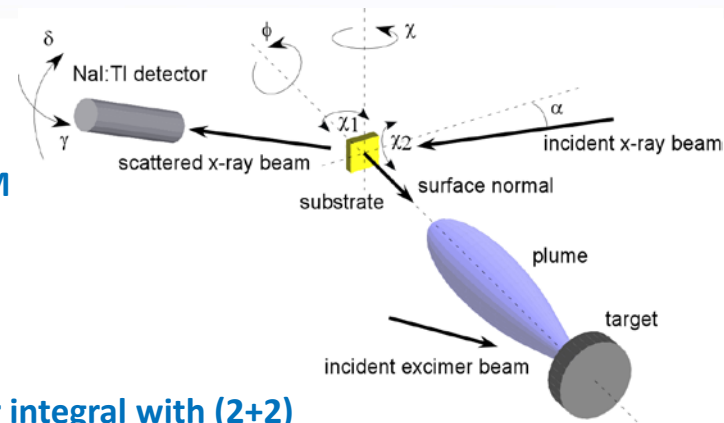
The PLD experimental apparatus

Be EXIT WINDOW



INCIDENT X-RAY BEAM

EXCIMER LASER BEAM



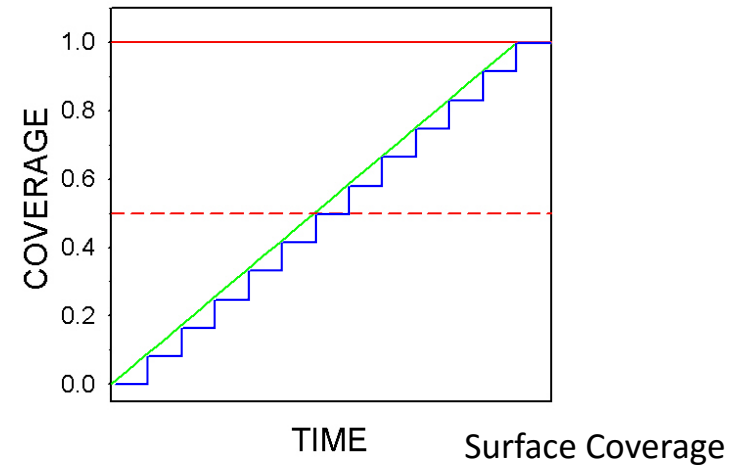
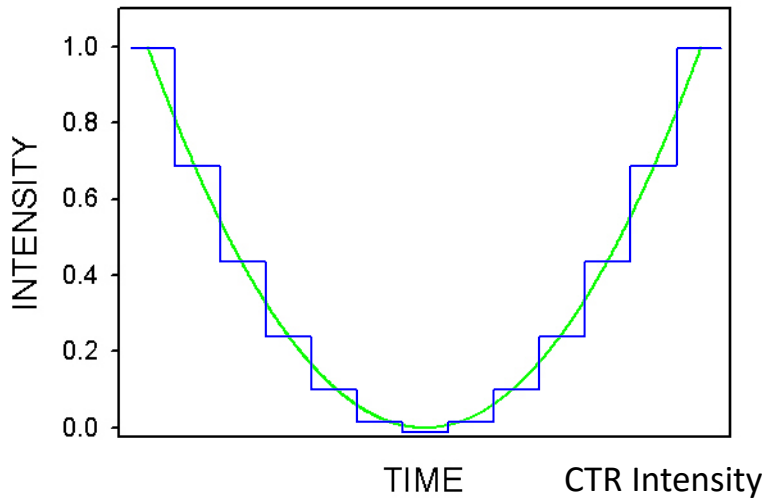
PLD chamber integral with (2+2) diffractometer optimized for surface diffraction.

- Epitaxy with very smooth surfaces at low growth temperature
- Excellent control of growth rate – multilayer and superlattice fabrication
- Simple operation process, low cost and no hazardous precursors required
- Exact stoichiometric transfer of materials from target to substrate - high quality complex films (eg. YBCO)
- Many growth parameters to control (laser parameters, target, substrate, pressure)

Signatures of ideal pulsed growth

- Continuous growth (eg: MBE) vs ideal pulsed growth
- PLD is very similar to ideal pulsed growth

$$I=(1-2\theta)^2$$

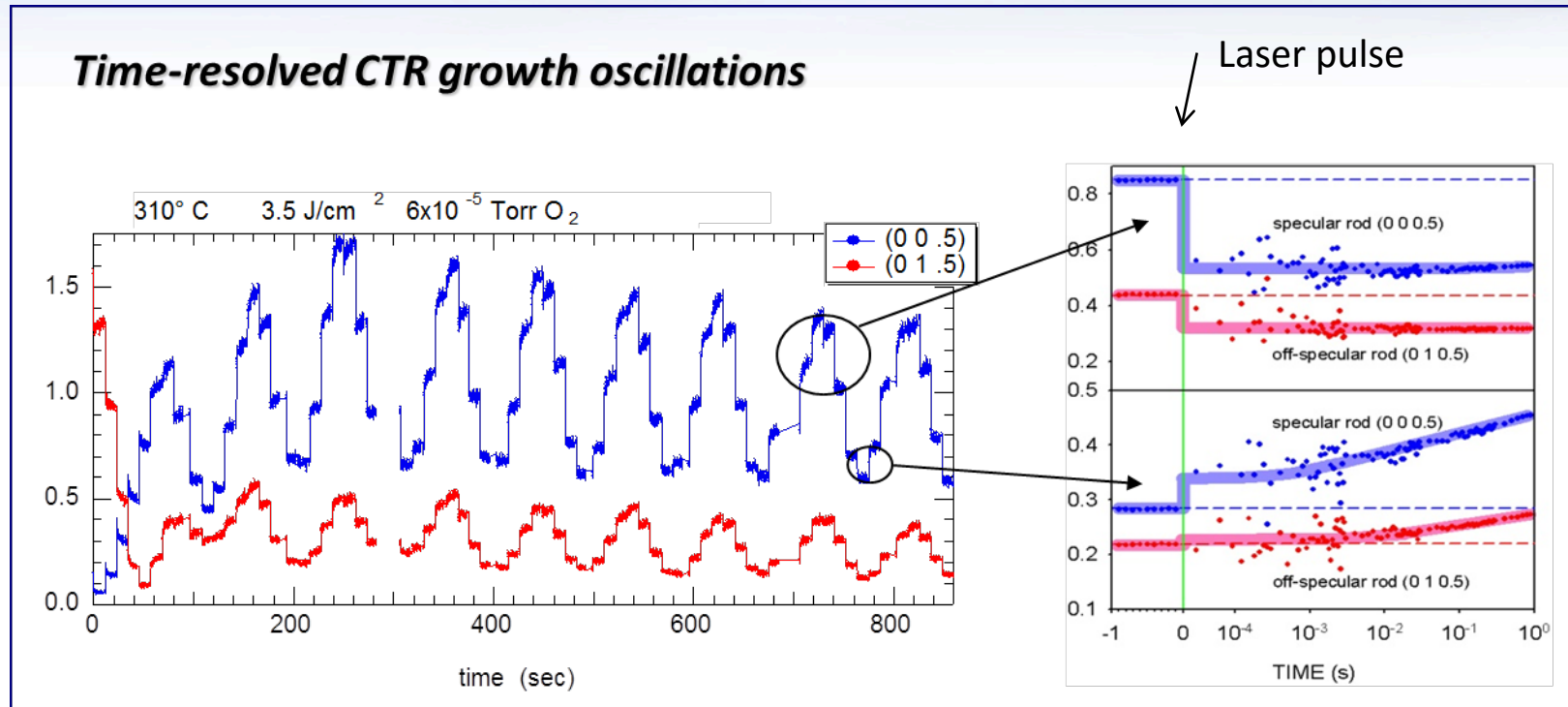


THEORETICAL WORK ADDRESSING PULSED GROWTH:

N. Combe and P. Jensen, PRB **57**,15553 (1998)

B. Hinnemann *et al.* PRL. **87**, 135701 (2001), PRE **67**, 011602 (2003)

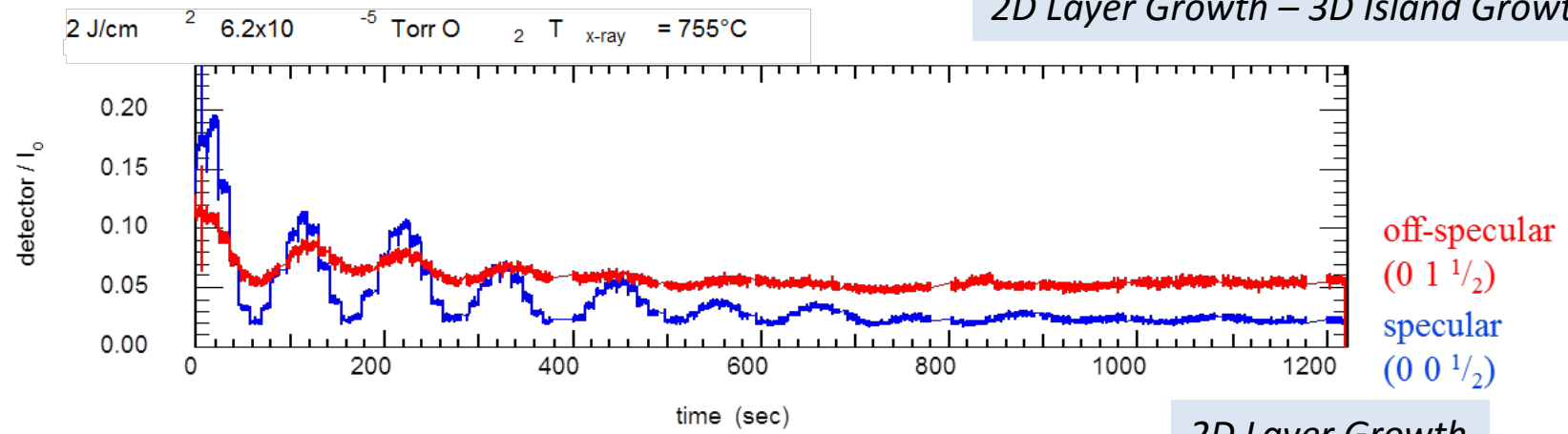
CTR oscillations during STO homoepitaxial growth



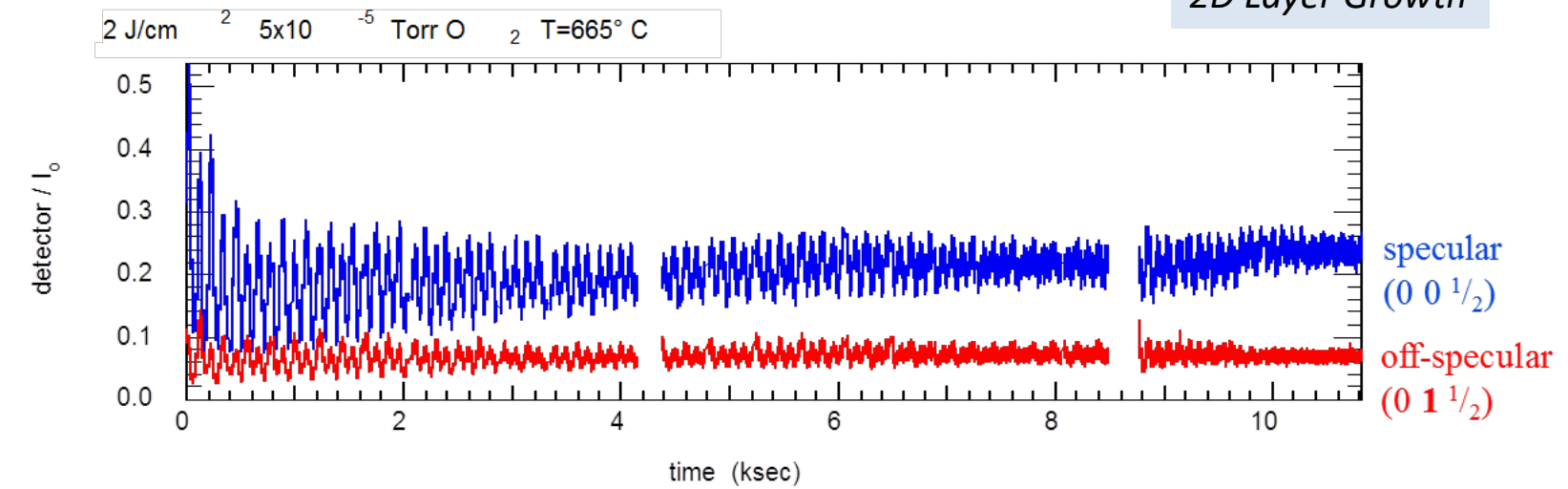
- Abrupt change in specular and off-specular rod intensity occurs simultaneously indicating crystallization occurs concurrently with the arrival of the ablated plume
- Abrupt change occurs faster than current measurement time resolution
- The mechanism of energy enhancement remains elusive and requires further study with improved time resolution – better than current 2-5 msec.

Temperature effect on growth mode

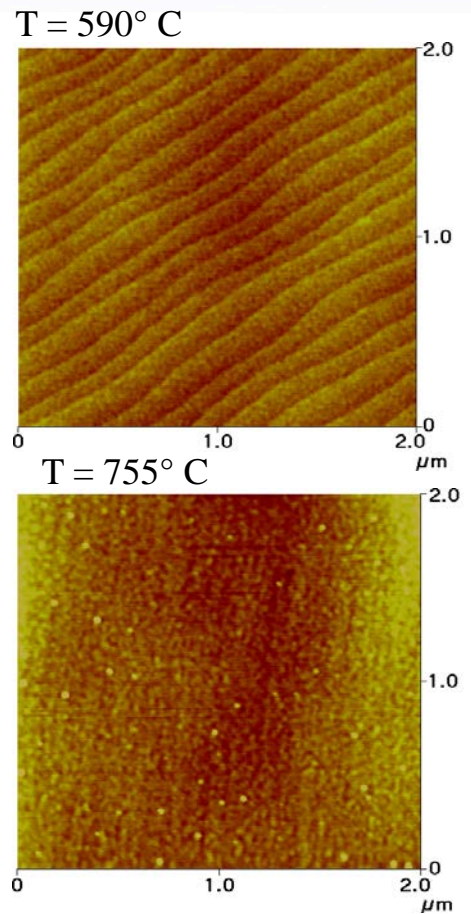
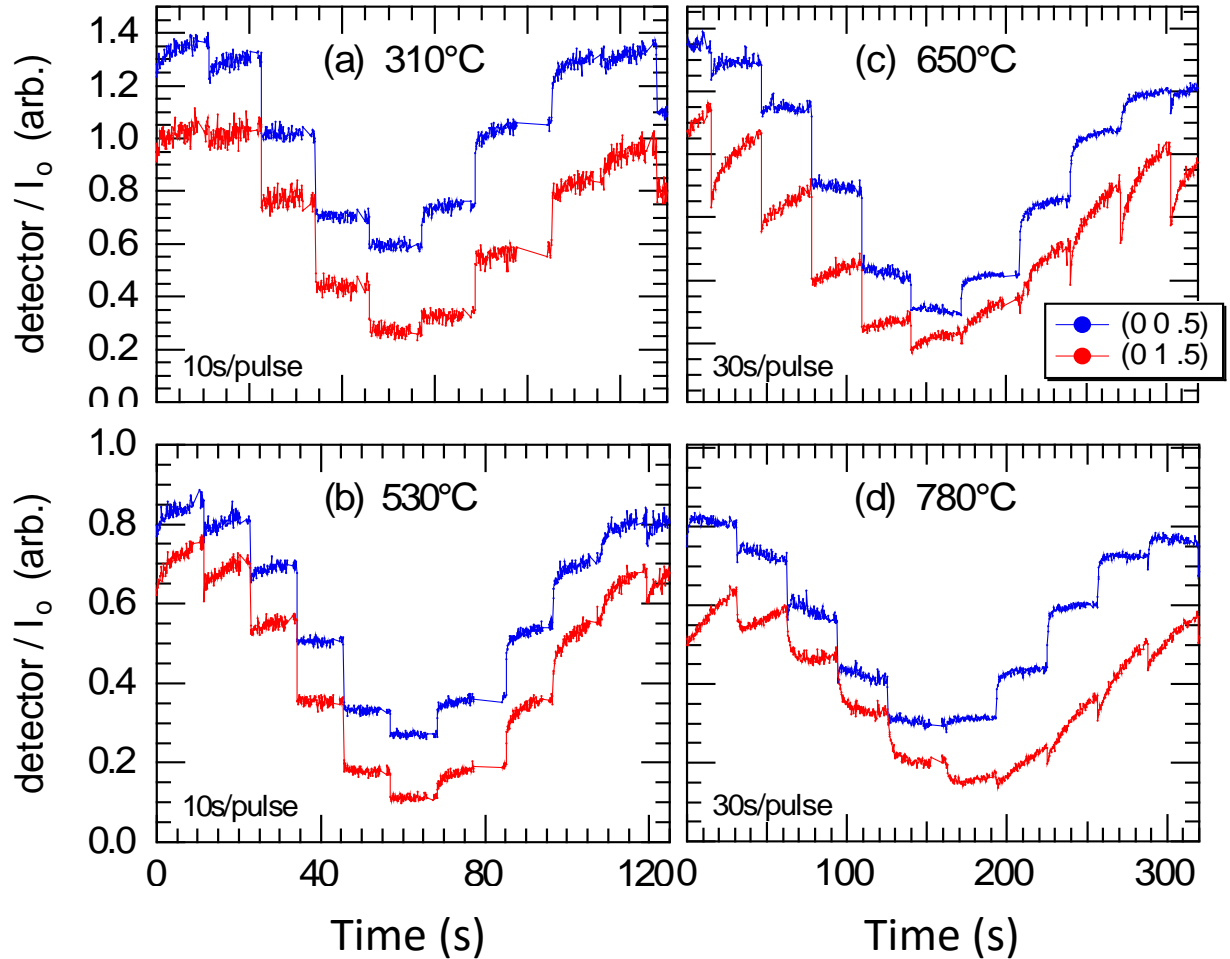
2D Layer Growth – 3D Island Growth



2D Layer Growth



Effect of temperature on in-plane order

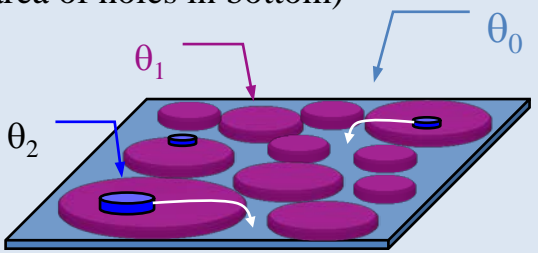


Simple model used for slow decay

- Model does not depend on any specific transport model

Rate ~ (material on level 2) x (area of holes in bottom)

$$\theta_2' = -\frac{\theta_2(t)\theta_0(t)}{\tau}$$



Where. $b + \theta_2(t) = \theta_0(t)$ is the area of holes

$$b = 1 - [\theta_2(t) + \theta_1(t)] = 1 - \theta_{total}$$

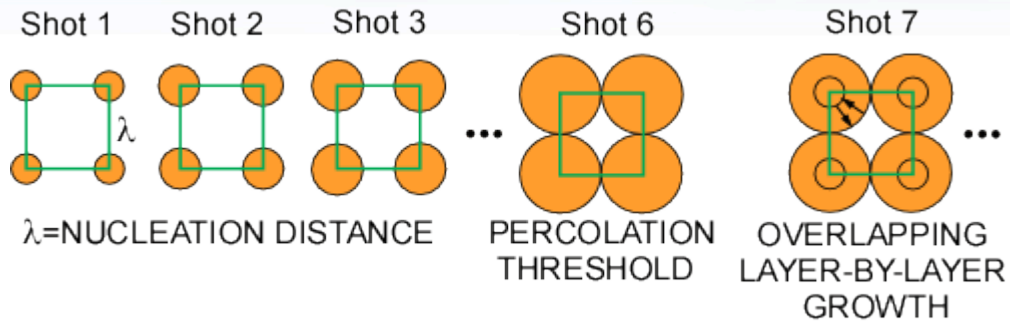
Solution to diff. eq.

$$\theta_2(t) = \frac{be^{bC}}{e^{bt/\tau} - e^{bC}}$$

Boundary condition

$$C = \frac{\ln\left(\frac{\theta_2(t=0)}{b + \theta_2(t=0)}\right)}{b}$$

Understanding Layer Formation

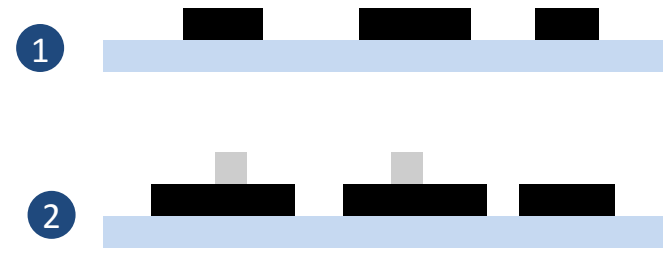
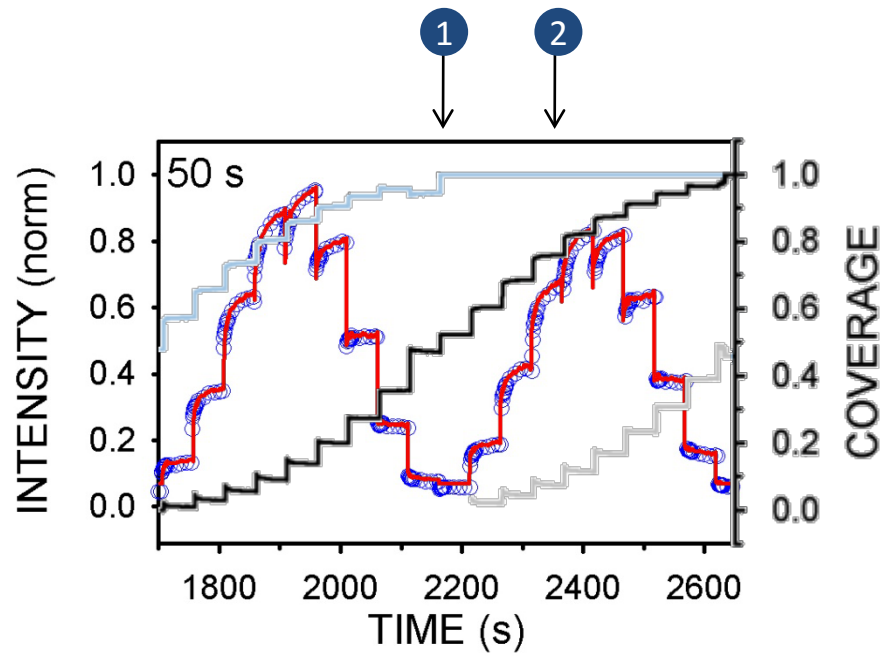


INSTEAD OF USING TRANSPORT MODELS TO FIT THE DATA WE EXTRACT THE TIME-DEPENDENT COVERAGES DIRECTLY FROM THE SXRD TRANSIENTS USING:

$$I(t) = I_0 [(1 - 2\theta_n(t) + 2\theta_{n+1}(t))]^2$$

$$\theta_n(t) + \theta_{n+1}(t) = \text{DEPOSITION PER PULSE}$$

THE TIME-DEPENDENT COVERAGES $\theta_n(t)$ AND $\theta_{n+1}(t)$ ARE NOT FLAT!



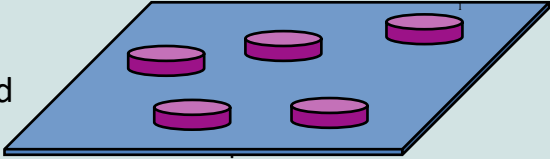
Tischler J. et al. PRL **96**, 226104 (2006)

Stable 2-layer growth

A Simple Conventional view

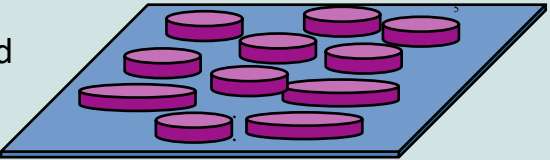
10 shots / layer shot #

$1/10$ covered 1



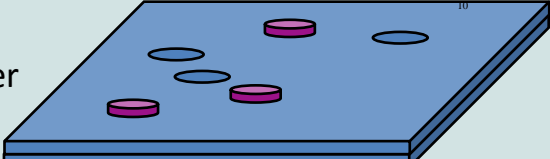
First shot has no interlayer transfer

$1/2$ covered 5



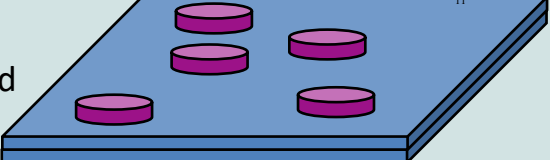
Rapid Interlayer transfer off half-coverage islands

1 monolayer 10



Sluggish Interlayer transfer due to long random walk, leaving ~5% holes + ~5% islands

$1 + 1/10$ covered 11

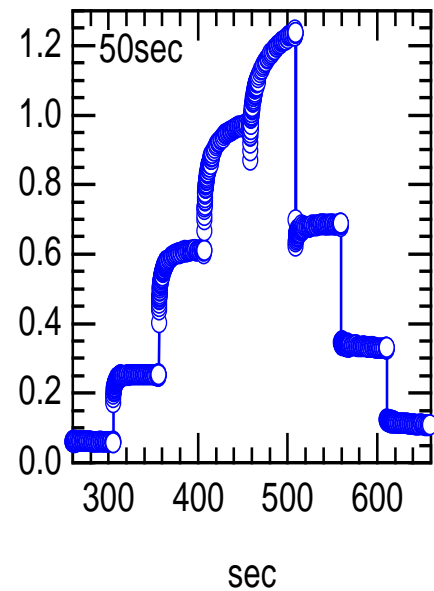
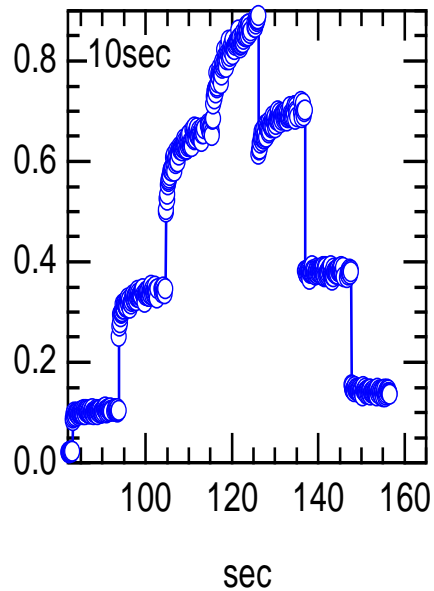
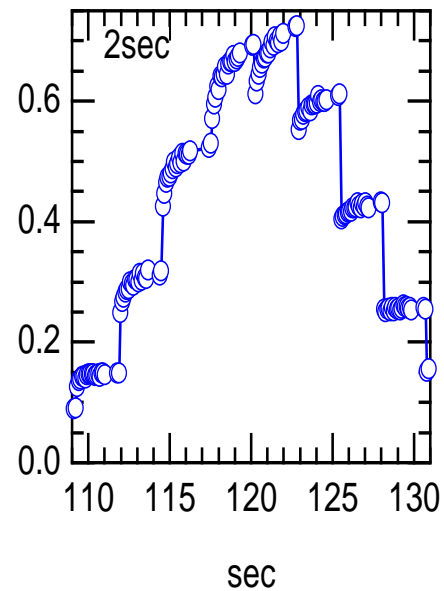
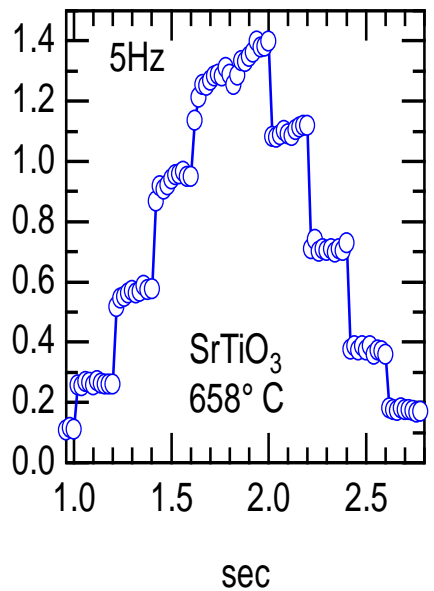
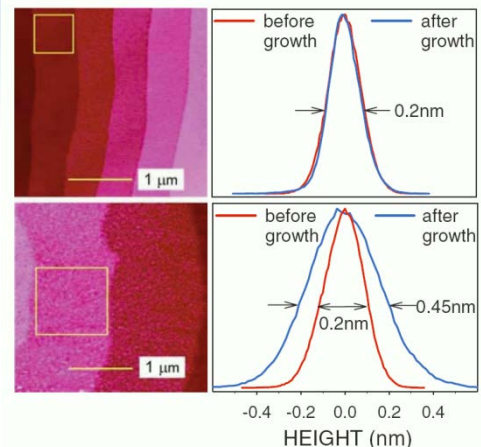


Shot 11 fills remaining holes and adds to new layer; Coverage the same as after shot 1.

Since the surface repeats, Growth proceeds without roughening

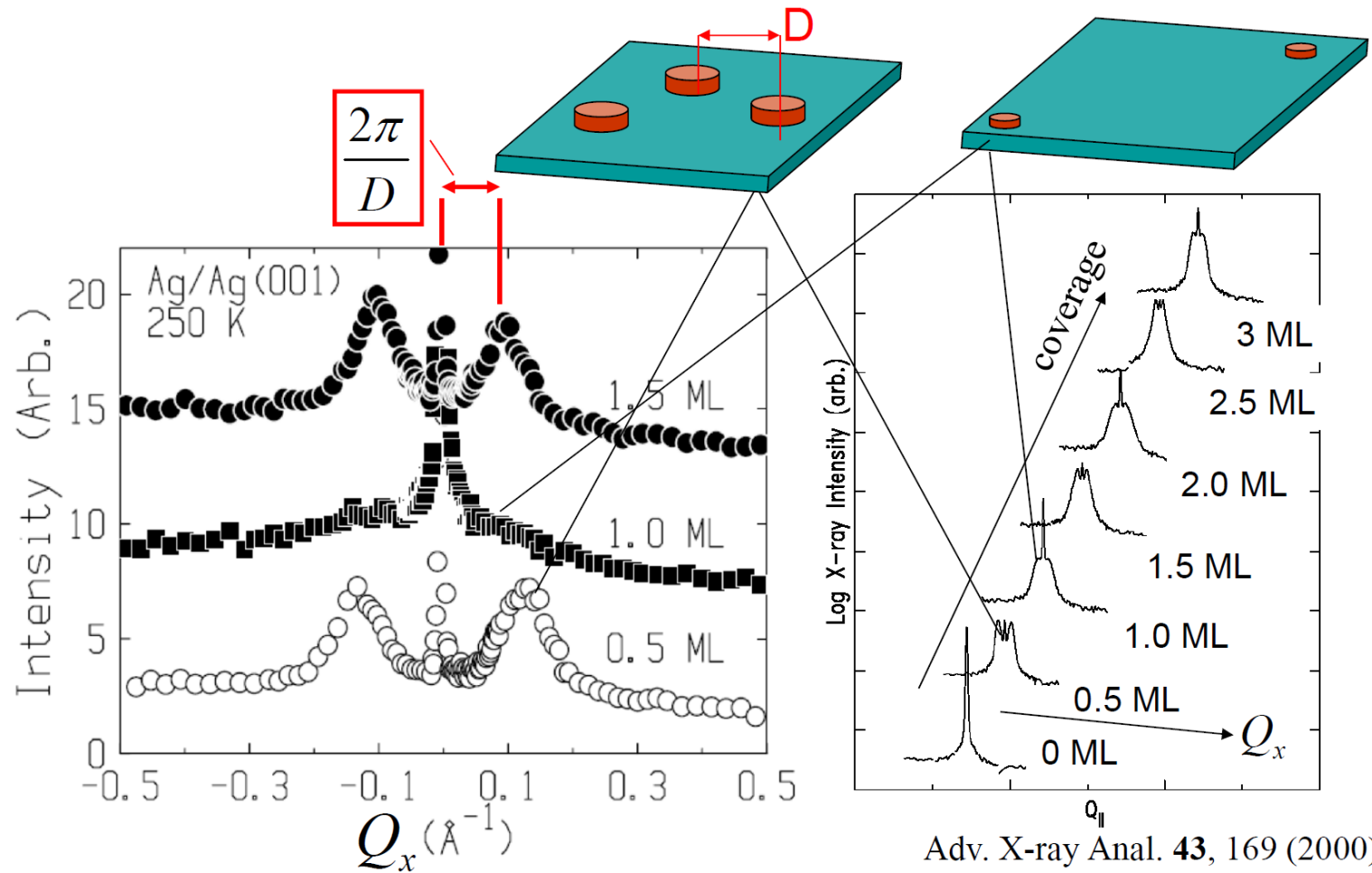
Self-similar in the time domain

- Dwell time between shots varies by x250, but 5Hz (0.2sec) data still shows rounding similar to 50 sec data (τ is changing). So sizes at 5Hz must be smaller than 50sec



Diffuse surface scattering from Ag during growth

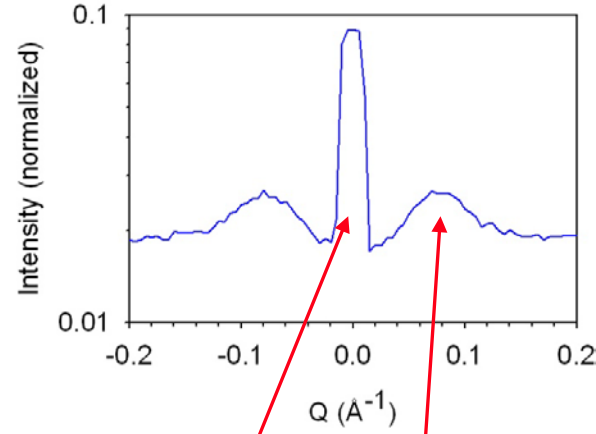
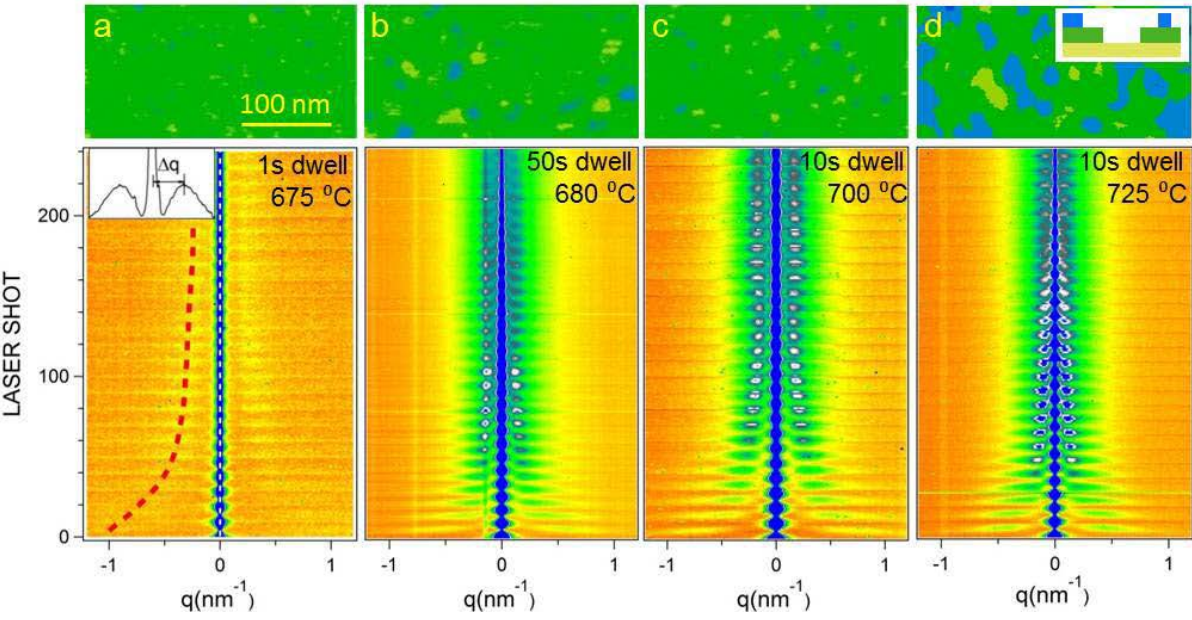
- Diffuse peak position contains correlation distance information
- Diffuse peak width relates to size distribution



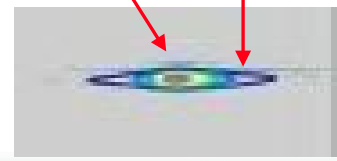
Adv. X-ray Anal. **43**, 169 (2000)

Island size evolution in STO PLD

- The island size and the spatial distribution of islands can be determined from the diffuse scattering component.
 - Diffuse peak position contains correlation distance information
 - Diffuse peak width relates to size and distribution
- Small island regime is at short dwell times and lower temperatures



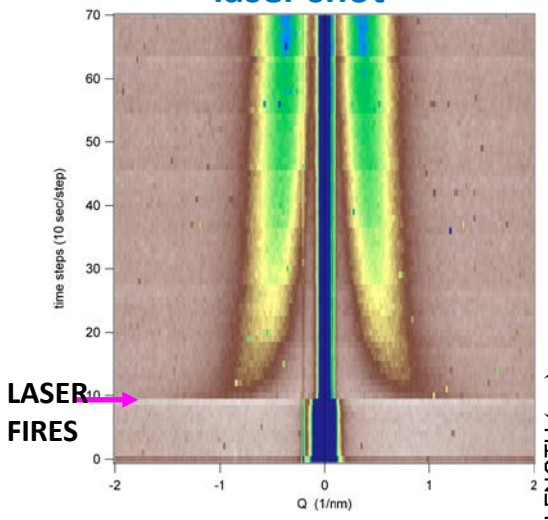
$$I(q) = I_{\text{coh}}(q) + I_{\text{diff}}(q) + I_{\text{backgr}}$$



Time-resolved diffuse x-ray scattering

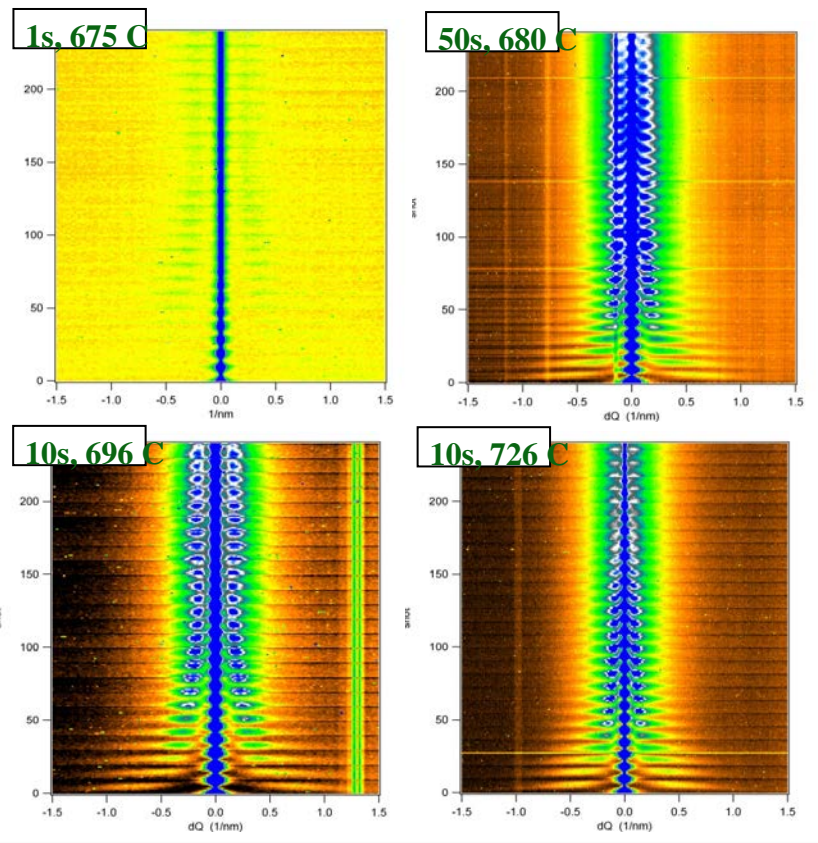
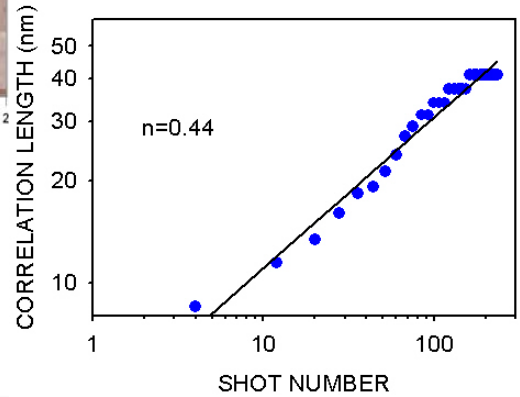
- Length-scale increases with substrate temperature at fixed dwell time
- Length scale increases with dwell time at fixed substrate temperature
- Need to understand the formation of a single layer

Diffuse scattering after a single laser shot



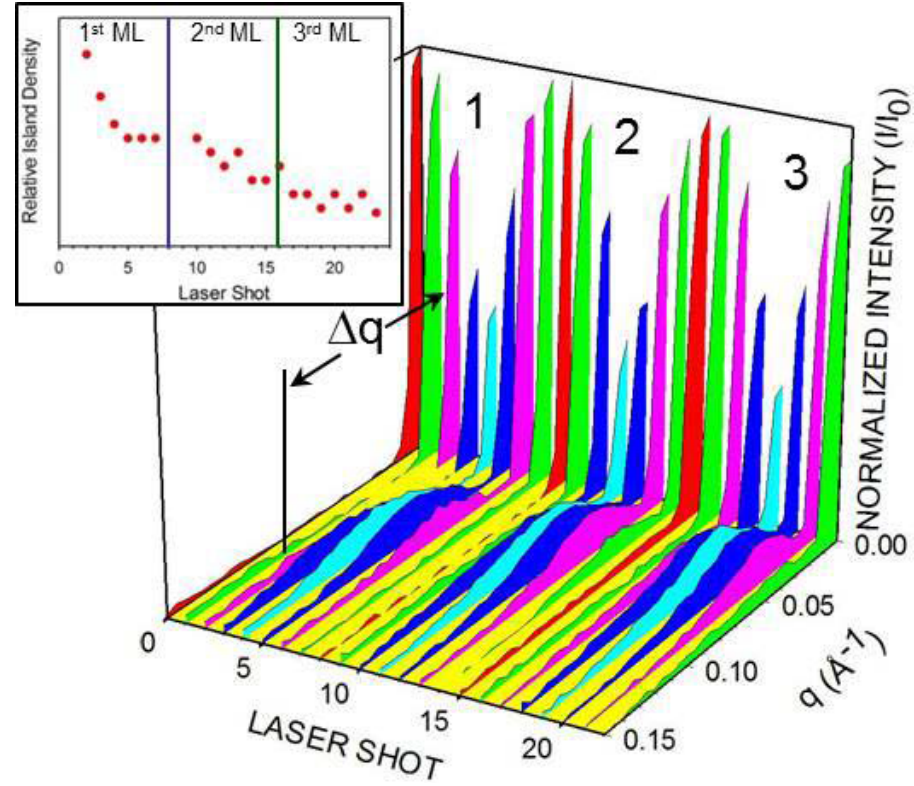
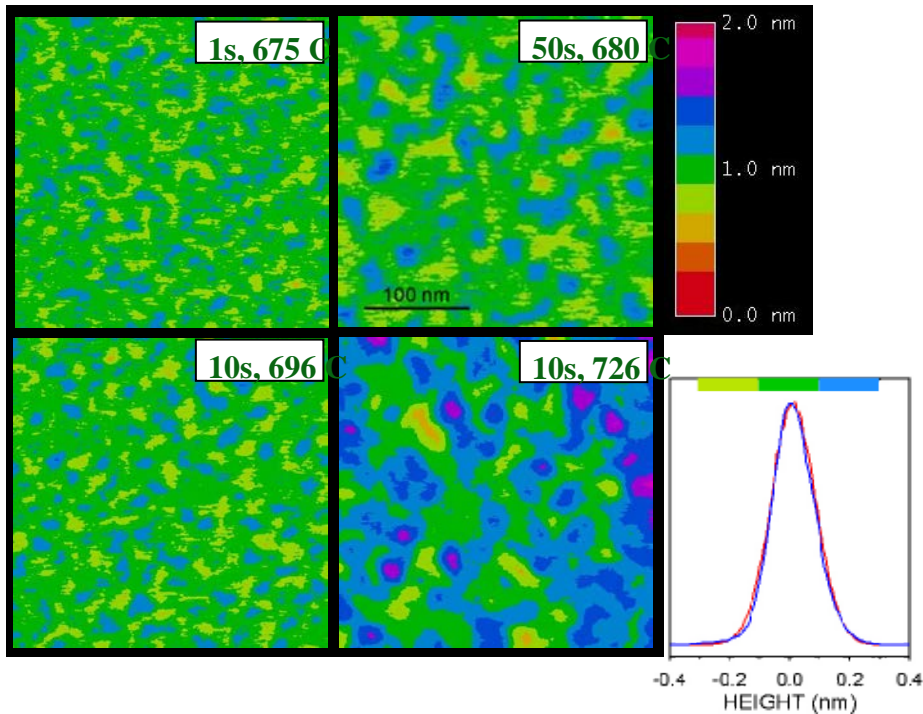
$$l(t) \propto t^n$$

$n =$ coarsening exponent
 $n = \frac{1}{3}$: diffusion-limited kinetics
 $n = \frac{1}{2}$: attachment-limited kinetics



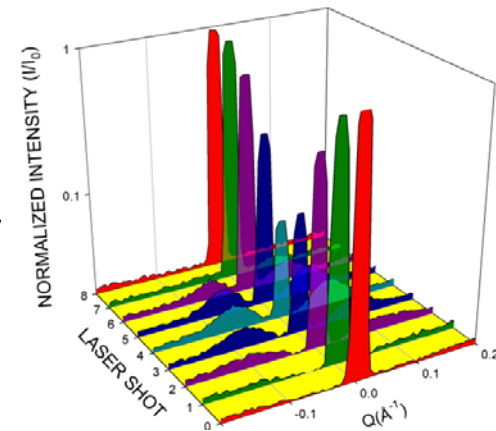
Real space imaging

- Length-scale increases with substrate temperature at fixed dwell time
- Length scale increases with dwell time at fixed substrate temperature



What have we learned about PLD growth?

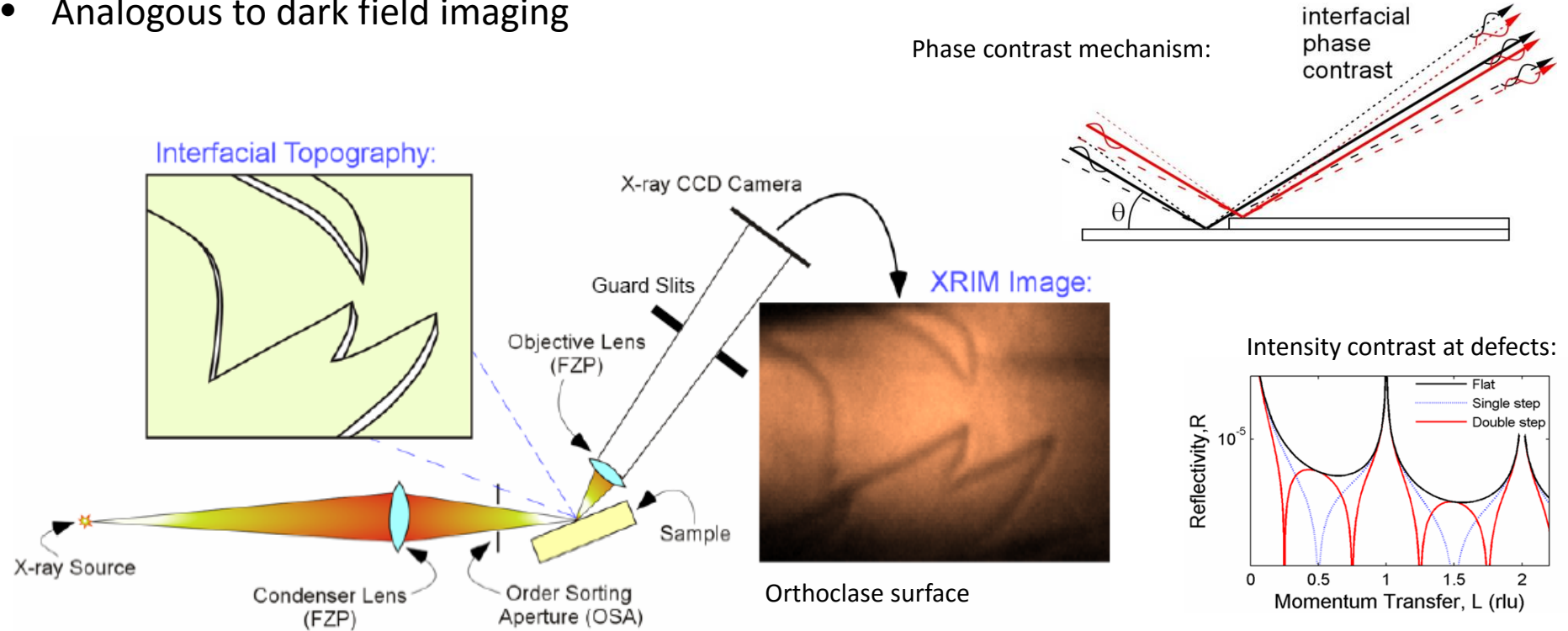
- Pulsed Growth permits separation of thermal & non-thermal effects
- In PLD, most of the material crystallizes in first few μs
- The thermal annealing affects less than 5 - 20% of the material deposited
- Stable 2-Layer growth established for SrTiO₃
- The transverse length scale depends upon Temperature and the dwell time between laser shots.
- Traditional models miss most of the physics.
- Heteroepitaxial systems behave similarly/differently



Tischler, et.al. *Phys Rev Lett* **96** (22) 226104 (2006)

X-ray Reflection Interface Microscopy (XRIM)

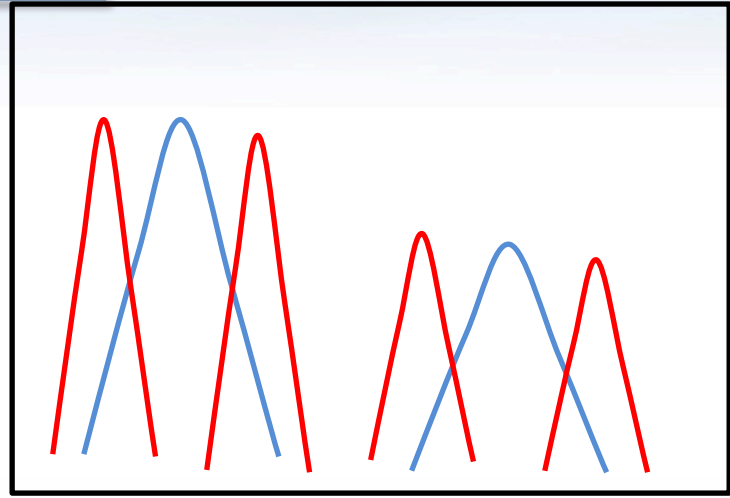
- Rather than measure the CTR intensity, imaging the scattered beam gives rise to interface microscopy
- Strong contrast (~100%), but weak reflected beam intensity ($R < 10^{-5}$)
- Sub-nm vertical sensitivity, but modest lateral resolution (~50-100 nm)
- Analogous to dark field imaging



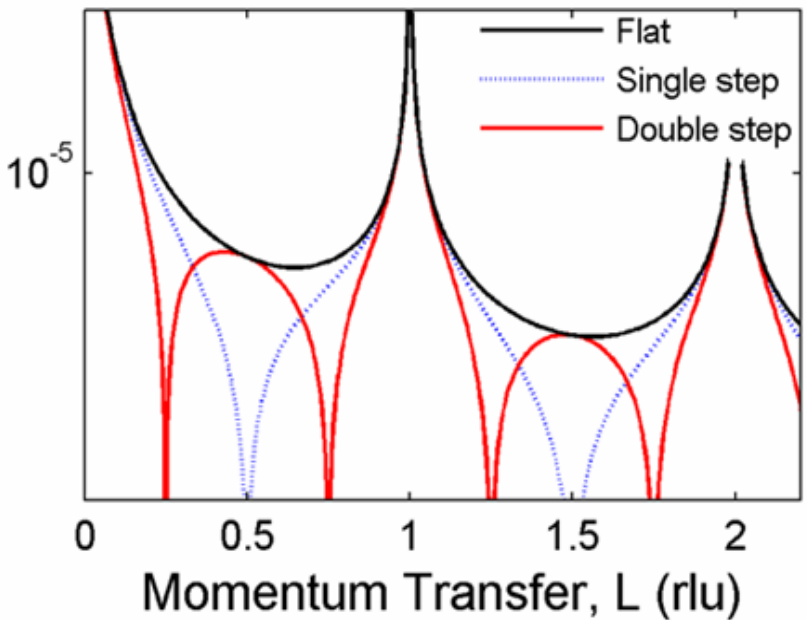
Fenter et al., *Nature Physics* 2(10) 700-704 (2006)

Contrast vs Q

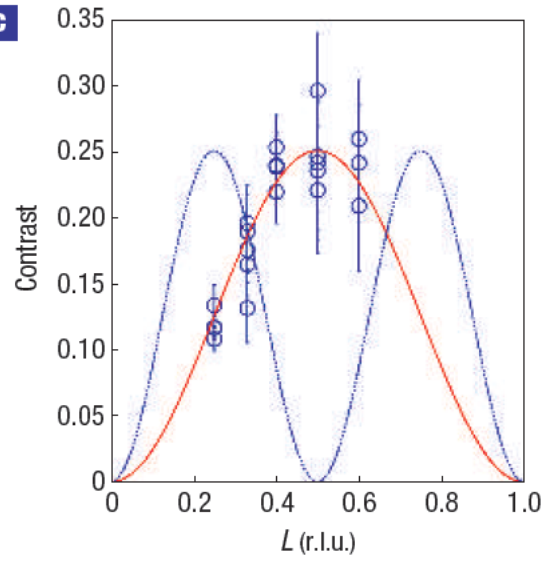
Contrast



Reflectivity, R

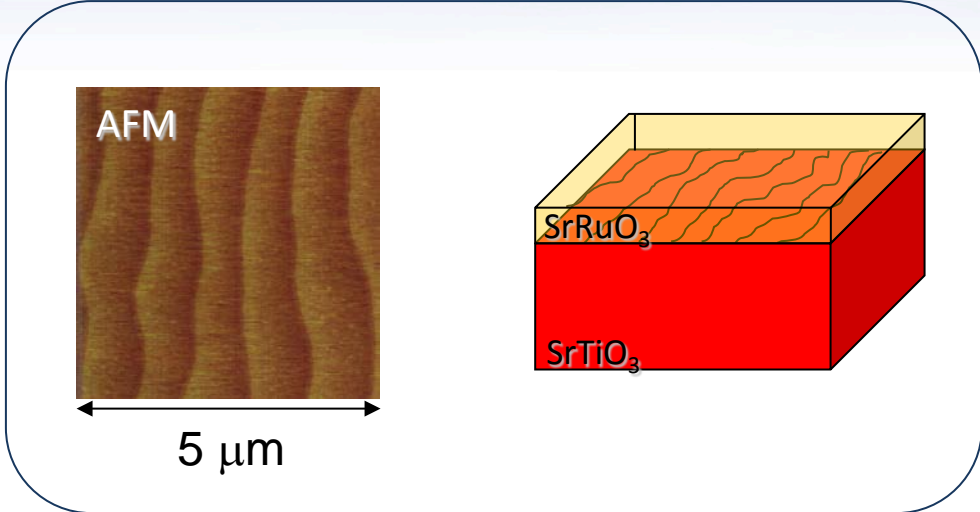


c

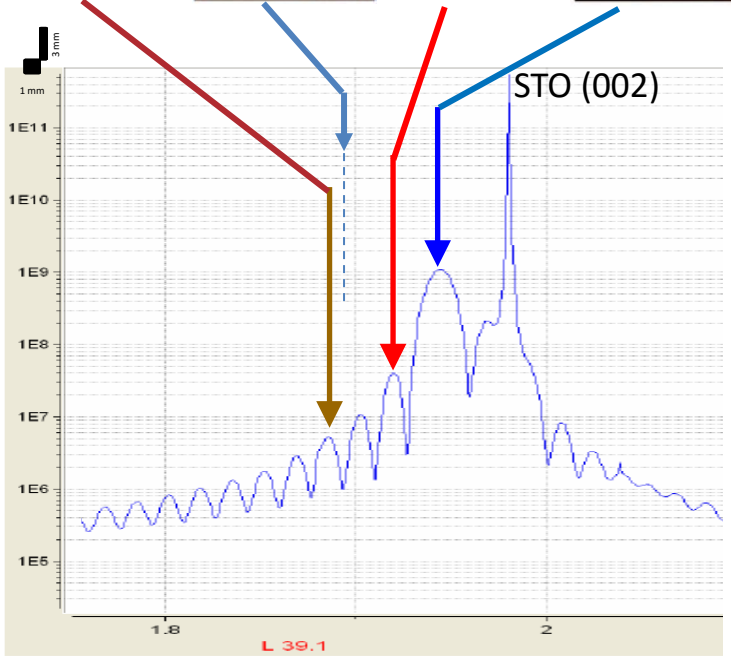
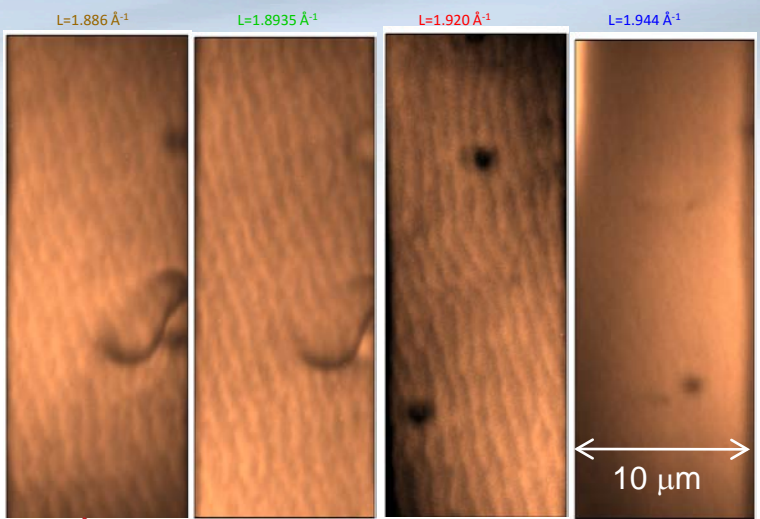


Fenter et al., *Nature Physics* 2(10) 700-704 (2006)

XRIM from buried interfaces

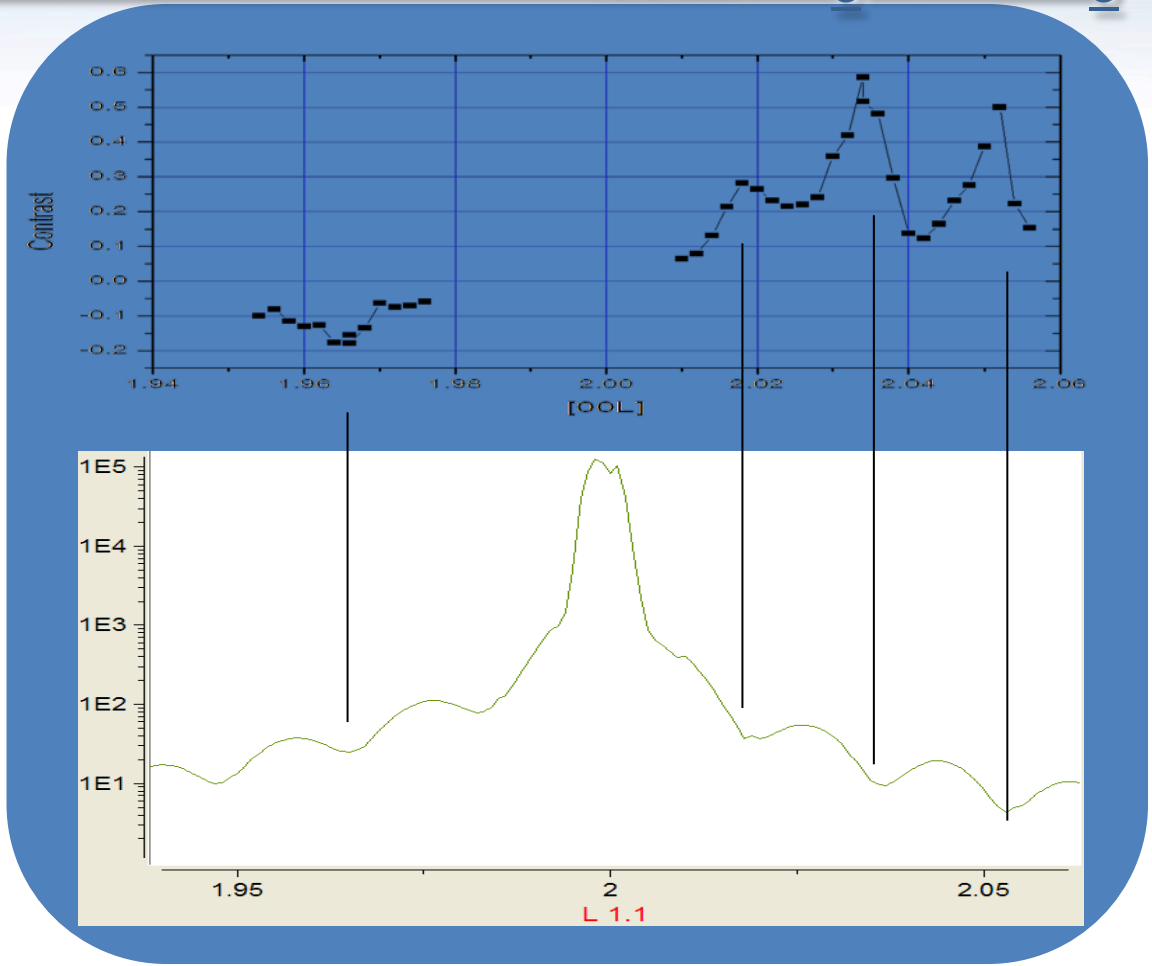


- In a thin-film, thickness fringes carry information concerning the details of the top and bottom surface (interface)
- XRIM can be applied to spatially resolve features from thin-film surface and interface structures.

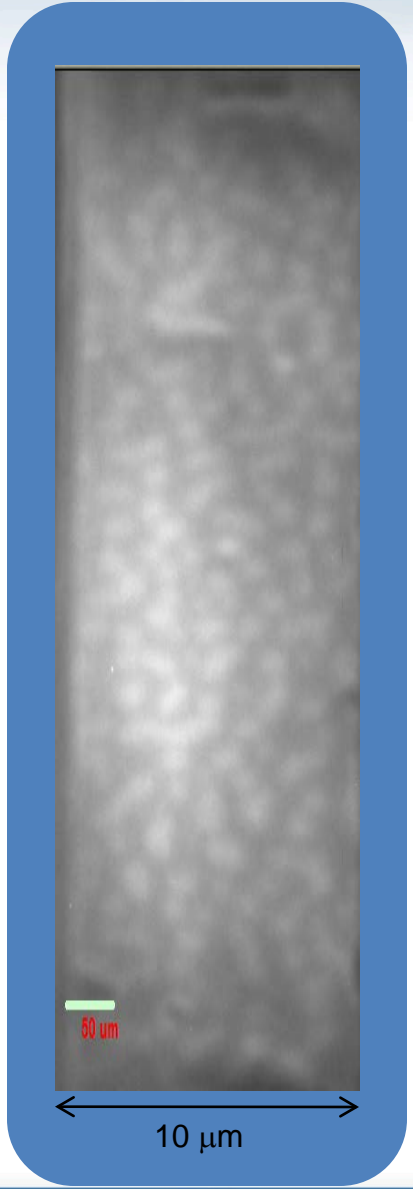


XRIM images of an interface between SrRuO₃ and SrTiO₃

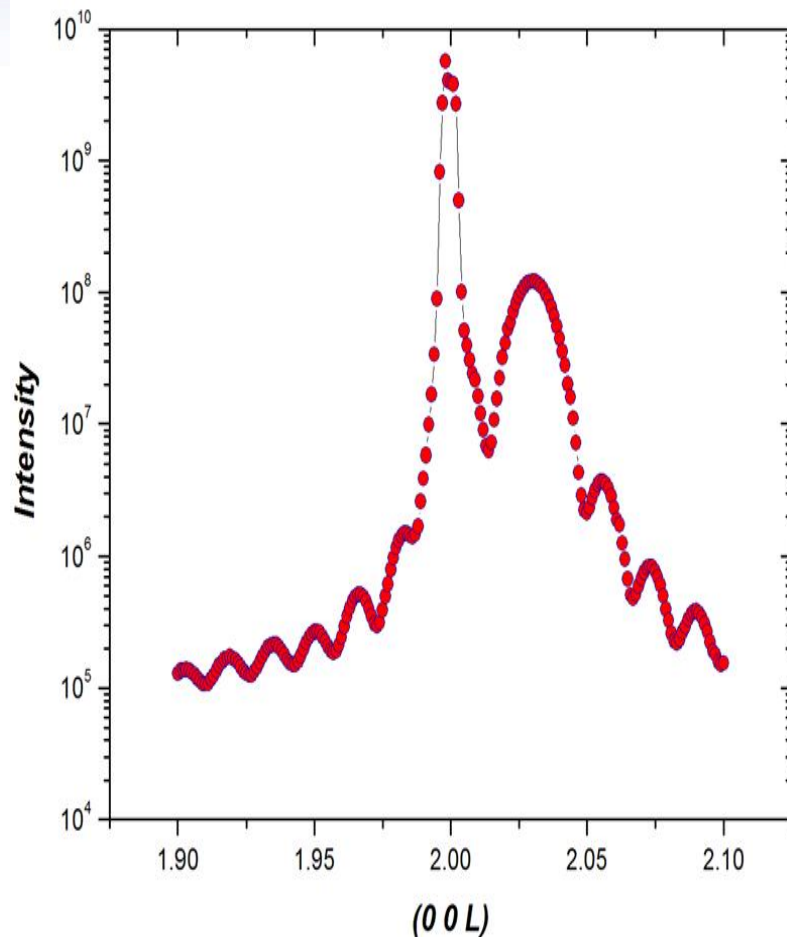
XRIM in Thin-Films: $\text{EuTiO}_3/\text{SrTiO}_3$



- Contrast observed in these films phase separation or inhomogeneous strain



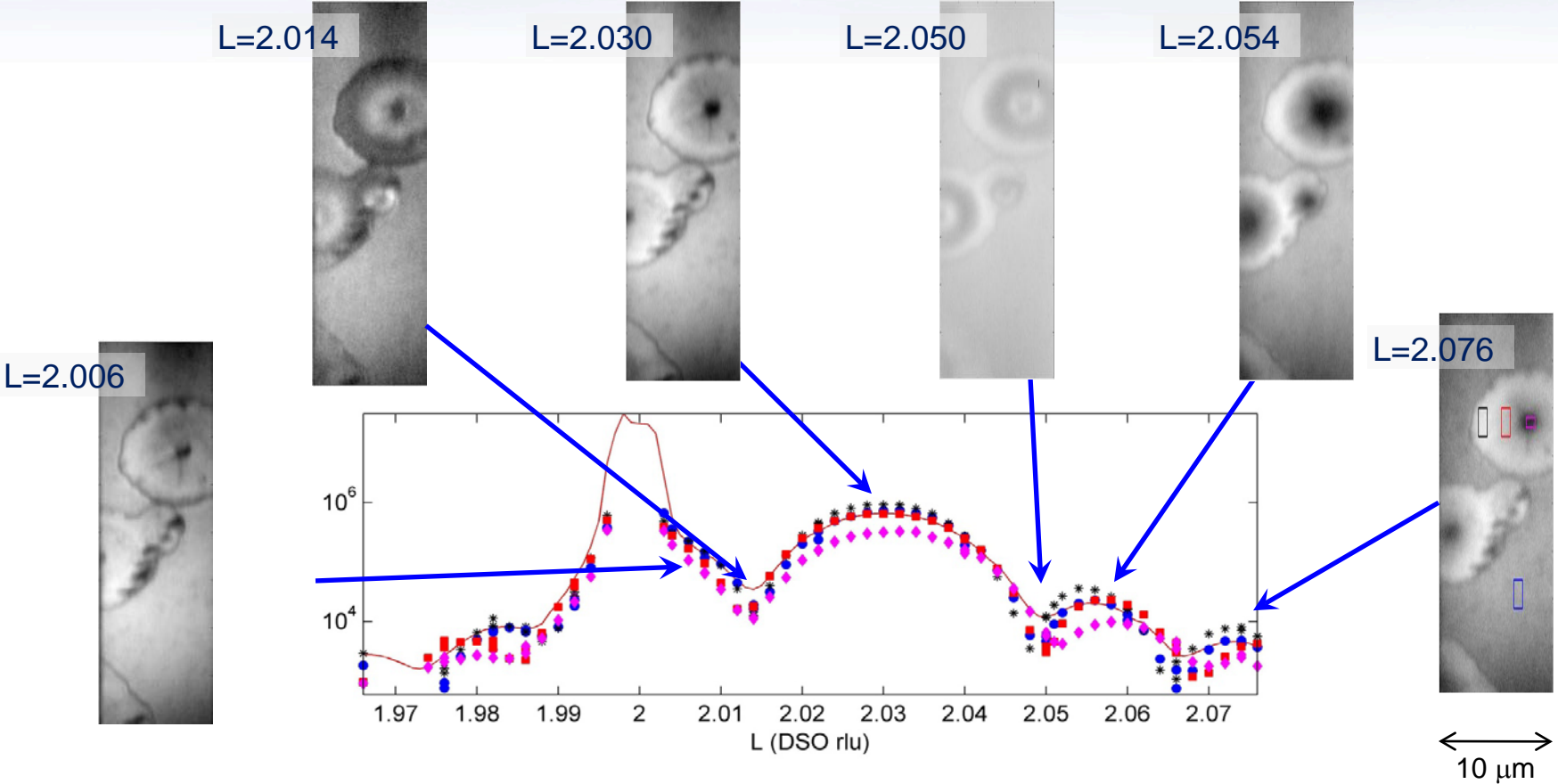
XRIM from a EuTiO_3 film on DyScO_3



Sample from June Hyuk Lee and Darrell G. Schlom (Cornell)

- Although a scattering measurement (left) shows a nice typical reflectivity curve, XRIM reveals that the film is not homogeneous.

XRIM in Thin-Films: $\text{EuTiO}_3/\text{DyScO}_3$

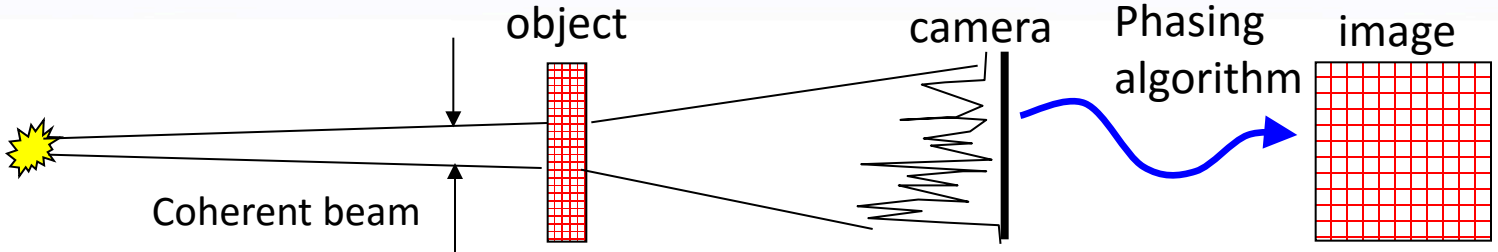


- Structure information with high spatial resolution can be obtained with quantitative analysis of the XRIM images.
- The center of the circular structure is thinner than the film average

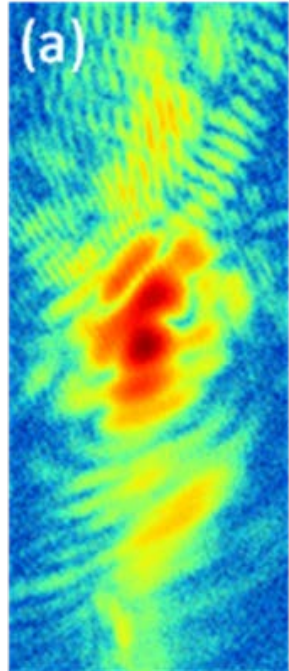
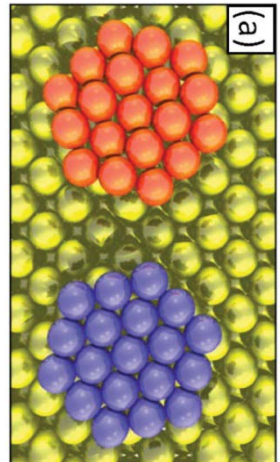
What have we learned from XRIM?

- XRIM holds great promise for in-situ real-time visualization (real-space) during materials growth and during chemical processes
- Sub-nanometer sensitivity to interface structures (normal) and 50 nm lateral spatial resolution expected.
- Value in combining both scattering (reciprocal space) with imaging (real space)

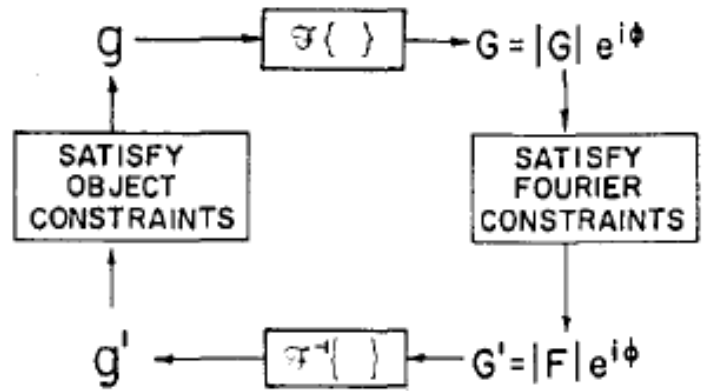
Coherent diffraction imaging of surface structures



“Coherent Diffraction pattern”



-robust phasing transforms scattering data to microscopic images

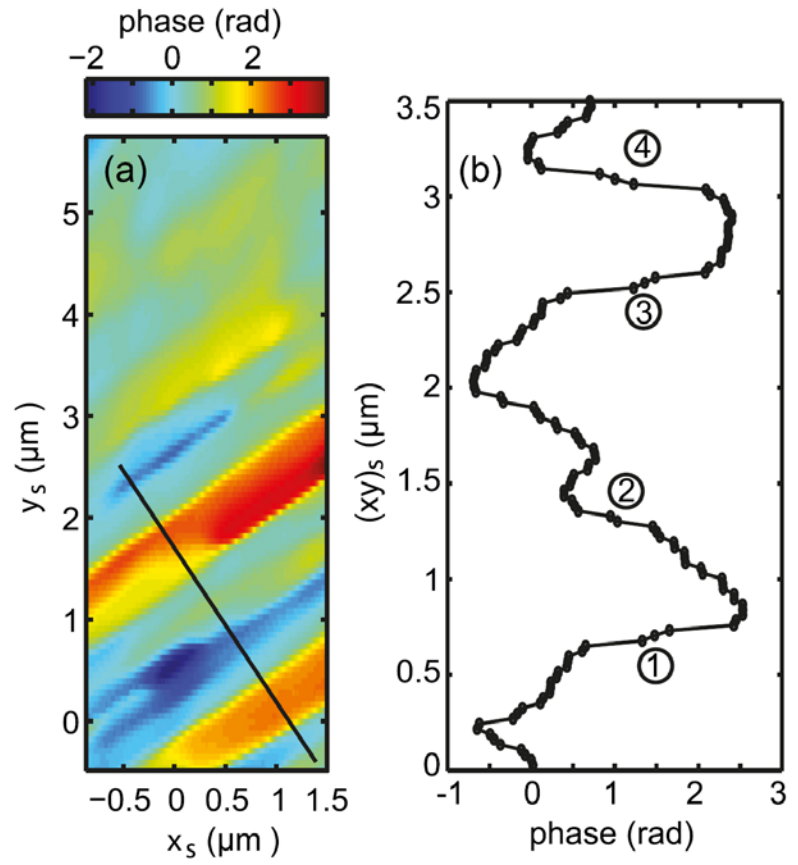
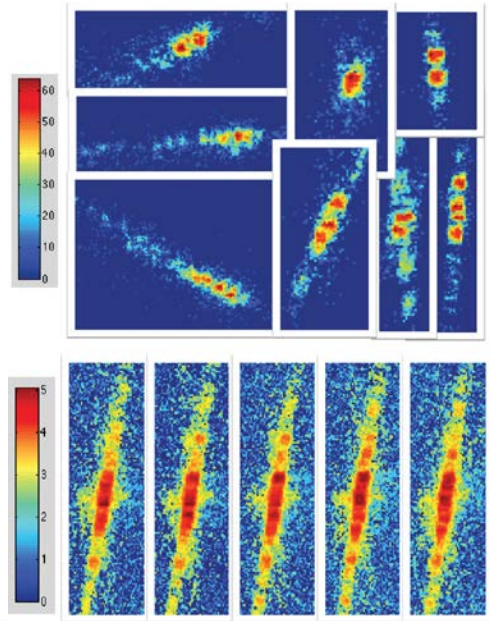
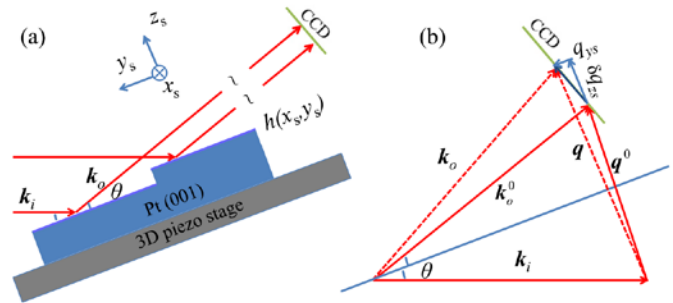


Fienup, Opt. Lett. 3, 27 (1978)

Au(001) Hexagonal reconstruction peak:
Pierce et al., unpublished results (2008)

Coherent diffraction imaging of steps on Pt (111)

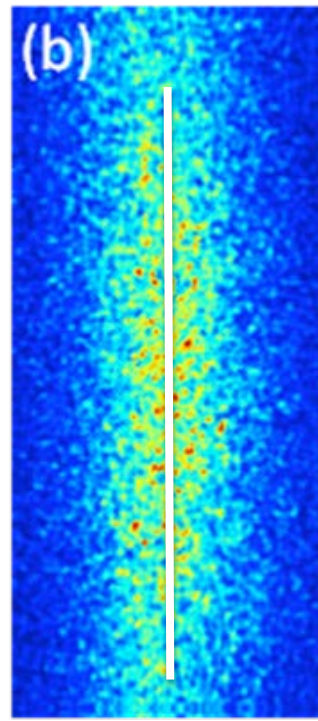
- Ptychography demonstrated to image step features on Pt (111) surface using coherent diffraction imaging



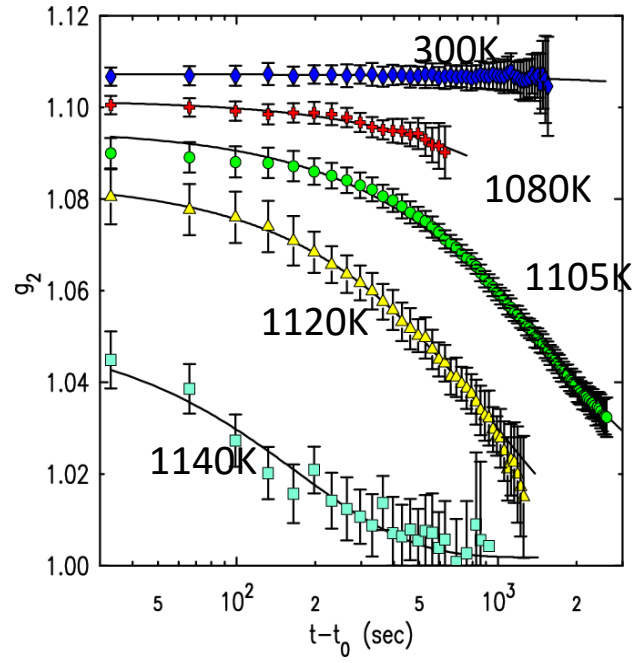
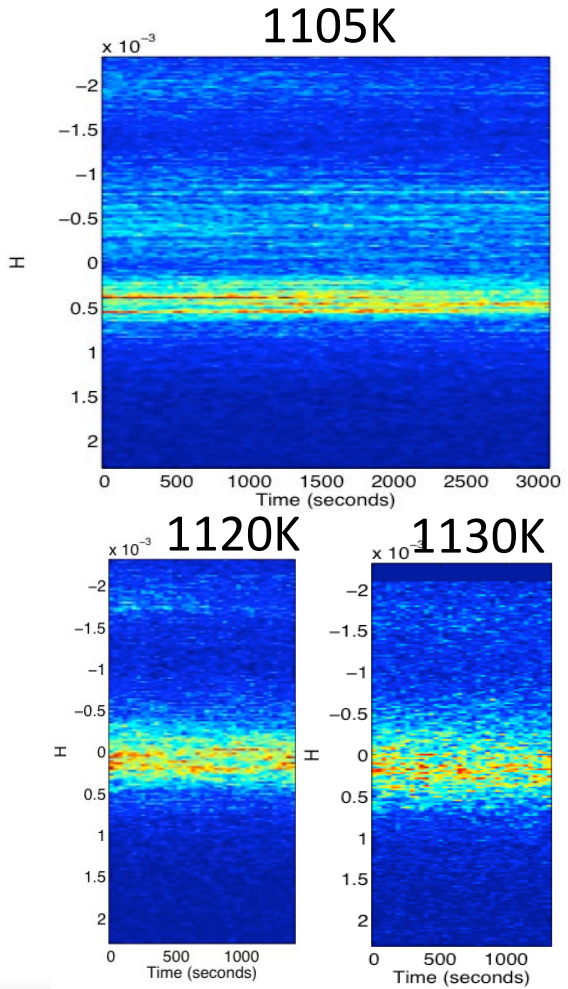
Zhu et al. Appl. Phys. Lett. 106, 101604 (2015)

Surface dynamics studied with XPCS - Au (001)

- Photon Correlation Spectroscopy exploits x-ray coherence to provide insight into surface dynamics



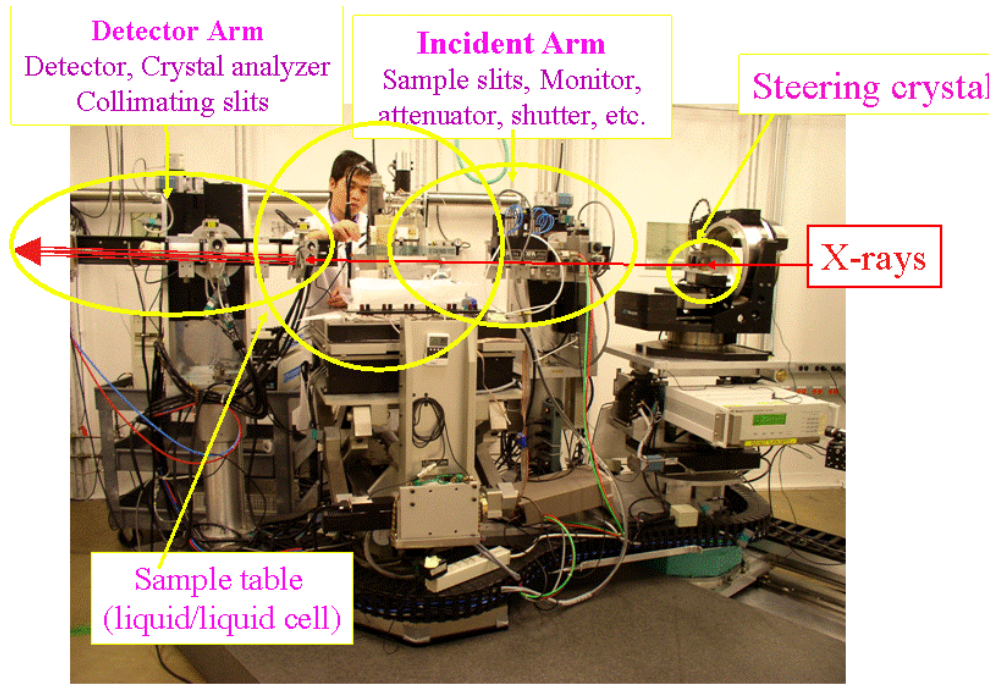
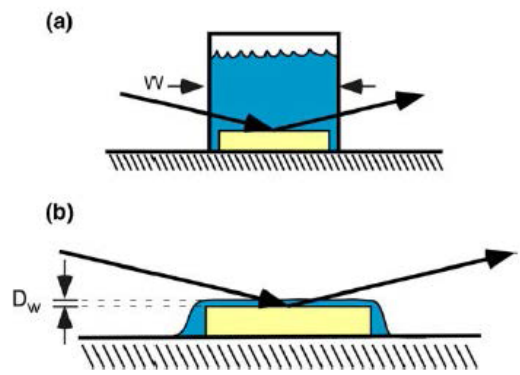
Au (001) CTR
(Anti-Bragg)



Pierce, et al., PRL 103, 165501 (2009)

Instrumentation

- Integrated diffraction – UHV growth chambers
 - Including RHEED, AUGER, LEED, XPS, sputtering, ellipsometry, etc...
- Liquid spectrometers
- Small Be dome environment
- Flow cells



Liquid surface spectrometer

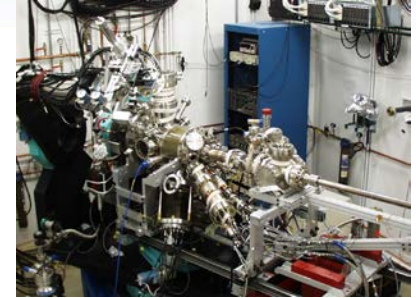
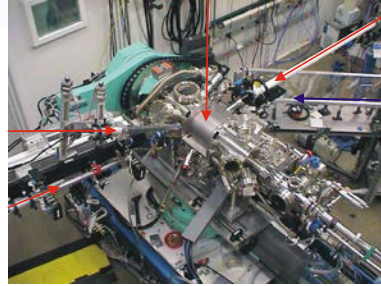
Interface Science facilities at the APS



13-ID surface scattering

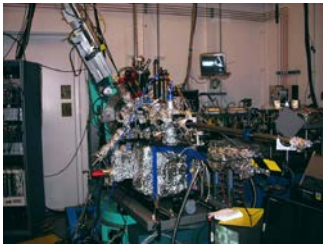


33-ID surface scattering , PLD, MBE

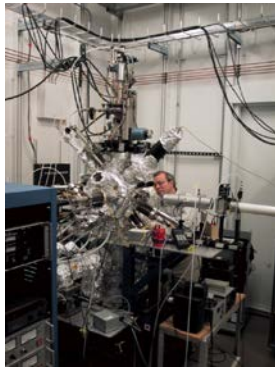


6 ID-C UHV surface scattering chamber

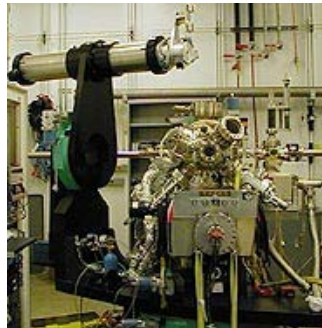
MBE-2



20-ID surface spectroscopy & diffraction



MBE-1



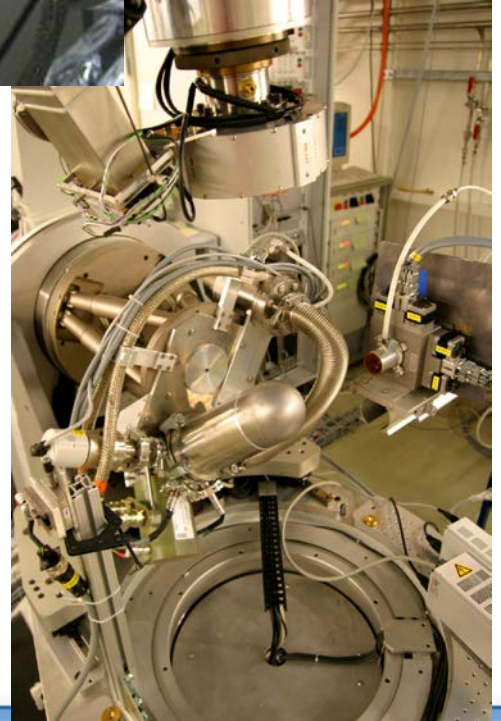
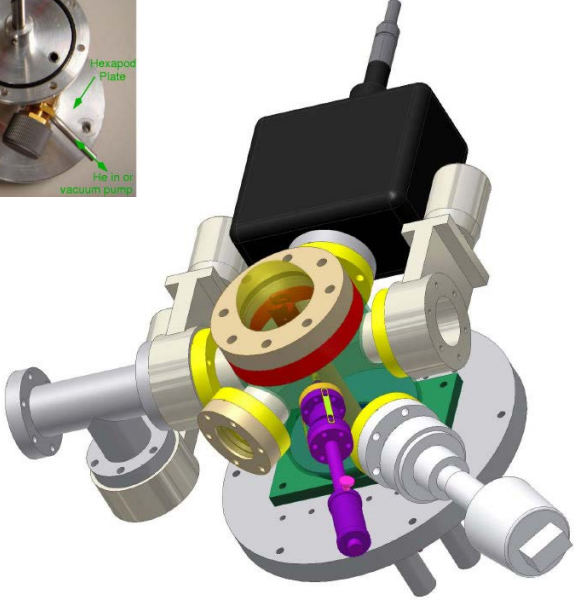
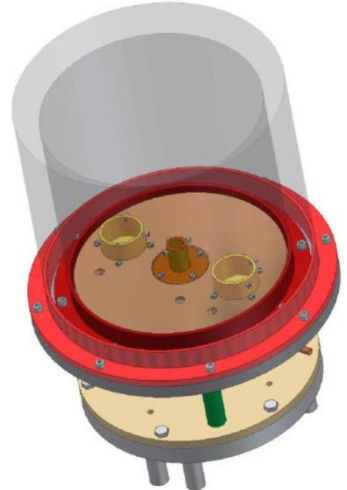
5 ID-C surface science chamber



12-ID surface scattering & MOCVD

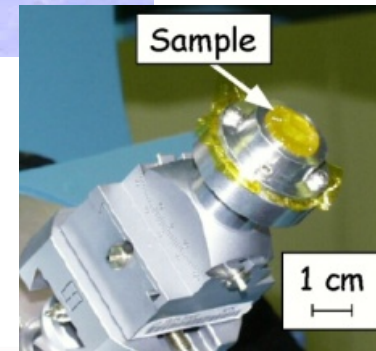
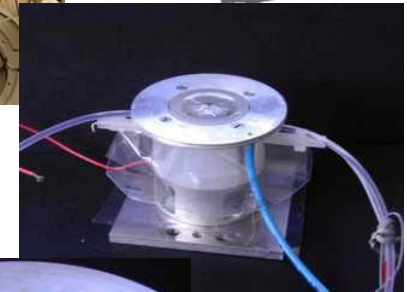
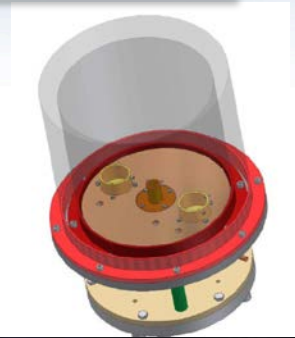
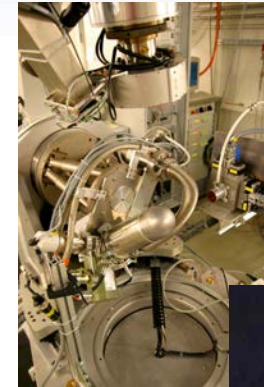
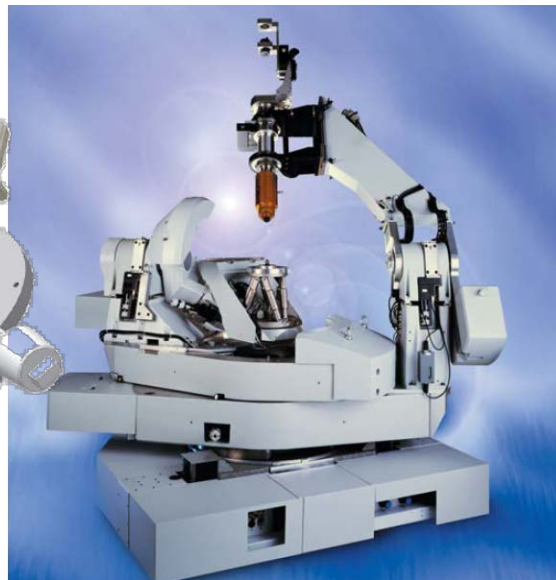
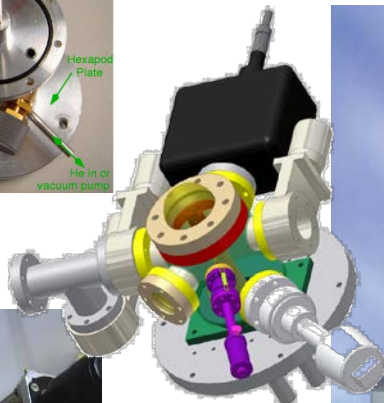
Small chamber approach at SLS & ESRF

- Ambient Chamber
- UHV baby Chamber
- Cryochamber
- High temperature system

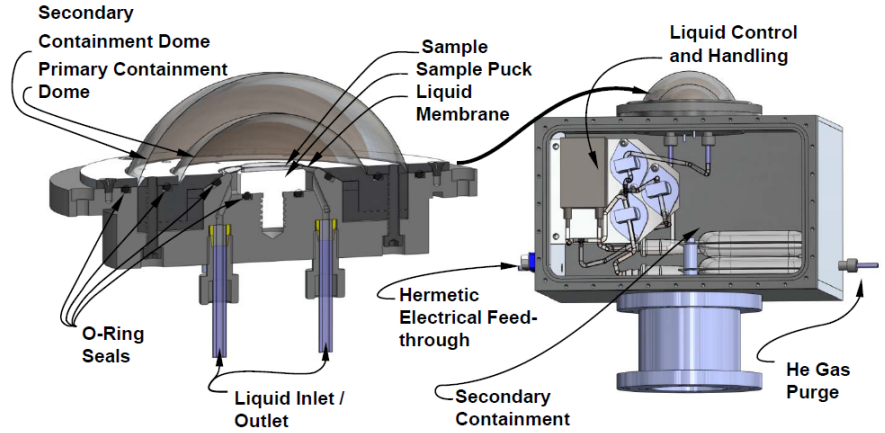
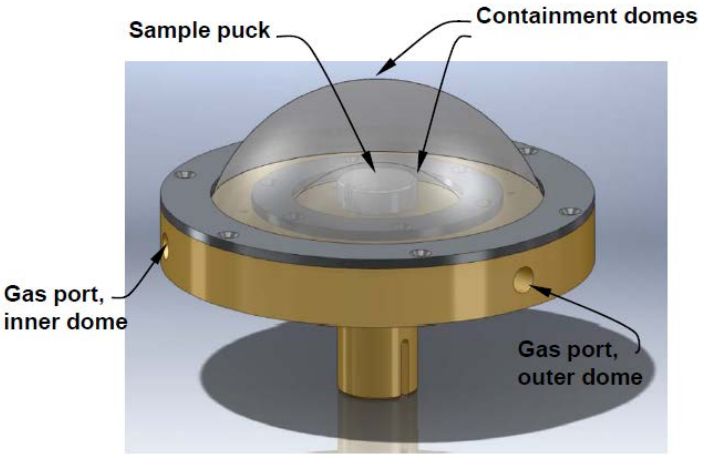
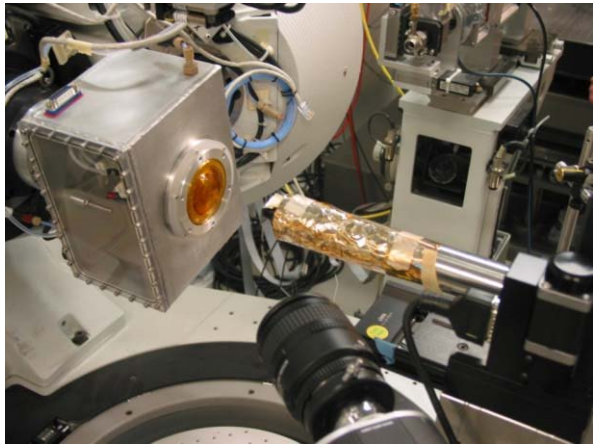
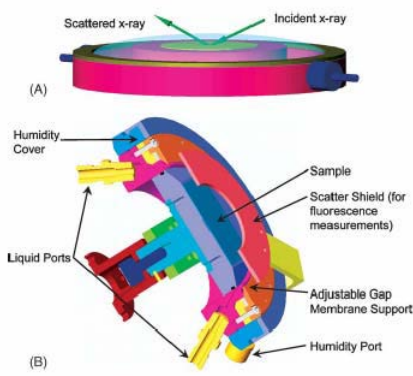


General diffractometers with sample environments

- Standardized interfaces interchangeable amongst diffractometers
- Environments include UHV, high-temperature, cryogenic, liquid flow-cells
- Enhanced general diffraction capabilities

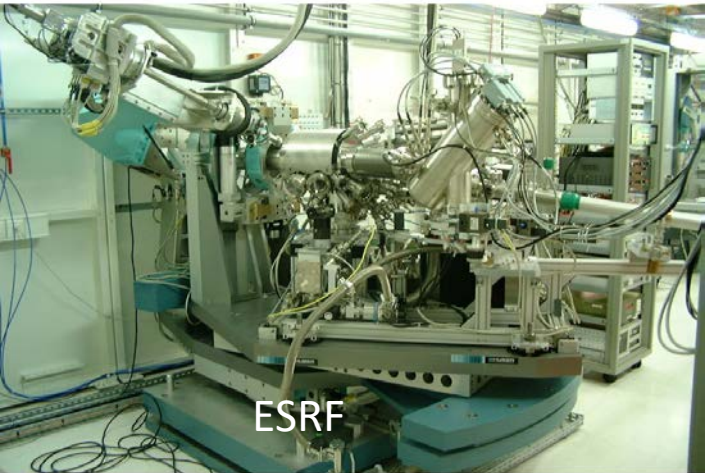
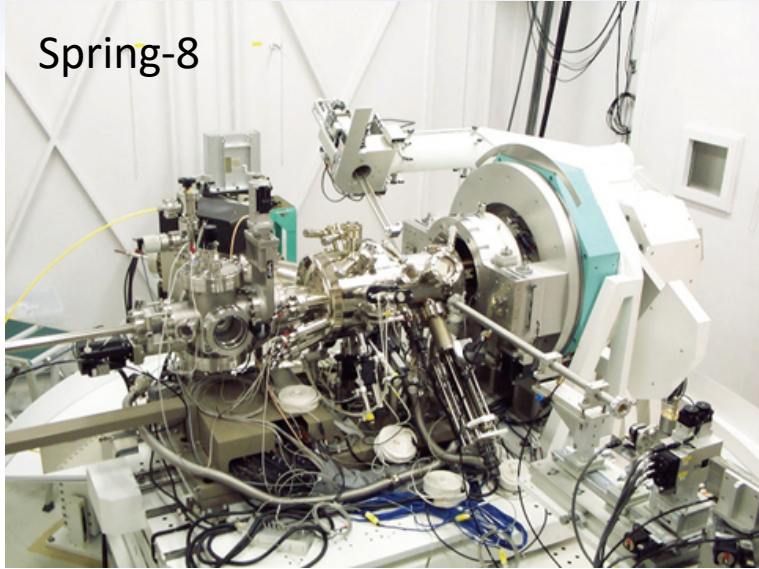
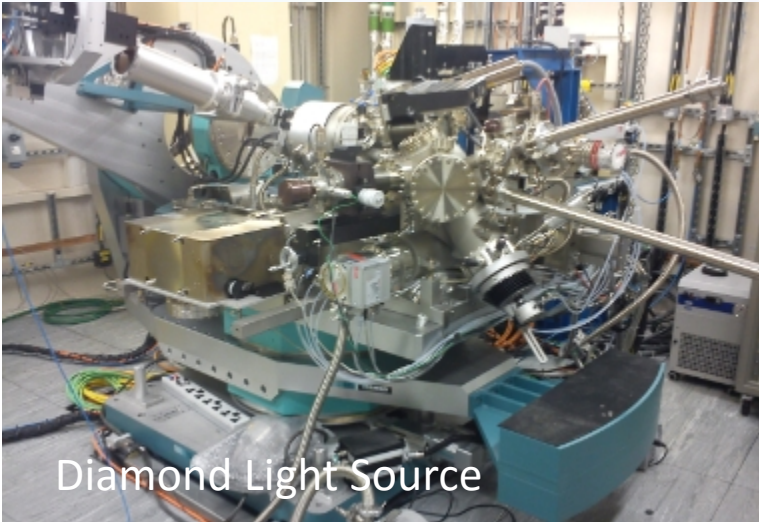


Sample environments to support interface science



Schmidt, Eng, Stubbs, Fenter, and Soderholm (2011) Rev. Sci. Inst. 82:075105

Most major Light Source facilities host interface science



Summary

- The origin of the Crystal Truncation Rod is the sharp termination of a lattice
- Crystal Truncation Rod scattering provides excellent sensitivity to surfaces and interfaces
- Widely diverse scientific communities exploit CTR techniques (materials synthesis, geosciences, catalysis, high-strength materials, electrochemistry)
- Learned how CTR scattering can be used to locate adsorbed species
- Demonstrated how time resolved CTR scattering can be used to study materials growth
- The CTR provides x-ray contrast that is sensitive to surface/interfaces and this scattering can be imaged with XRIM
- Many advanced techniques applied to bulk materials can be applied to interfaces through exploitation of the CTR (XPCS, CDI, diffuse scattering)